
# VYSOKÉ UČENÍ TECHNICKÉ V BRNĚ
BRNO UNIVERSITY OF TECHNOLOGY

## FAKULTA STROJNÍHO INŽENÝRSTVÍ
FACULTY OF MECHANICAL ENGINEERING

## ENERGETICKÝ ÚSTAV
ENERGY INSTITUTE


# EXPERIMENTÁLNÍ STUDIE VLASTNOSTÍ SPREJE A FUNKČNOSTI MALÝCH TLAKOVÝCH VÍŘIVÝCH TRYSEK

EXPERIMENTAL STUDY OF SPRAY CHARACTERISTICS AND FUNCTIONALITY OF SMALL PRESSURE-SWIRL ATOMIZERS

DIPLOMOVÁ PRÁCE
MASTER'S THESIS


AUTOR PRÁCE
AUTHOR

Bc. Milan Malý

VEDOUCÍ PRÁCE
SUPERVISOR

doc. Ing. Jan Jedelský, Ph.D.



BRNO 2016

VYSOKÉ UČENÍ TECHNICKÉ V BRNĚ
FAKULTA STROJNÍHO INŽENÝRSTVÍ

# Zadání diplomové práce

| | |
|---|---|
| Ústav: | Energetický ústav |
| Student: | **Bc. Milan Malý** |
| Studijní program: | Strojní inženýrství |
| Studijní obor: | Technika prostředí |
| Vedoucí práce: | **doc. Ing. Jan Jedelský, Ph.D.** |
| Akademický rok: | 2015/16 |

Ředitel ústavu Vám v souladu se zákonem č.111/1998 o vysokých školách a se Studijním a zkušebním řádem VUT v Brně určuje následující téma diplomové práce:

## Experimentální studie vlastností spreje a funkčnosti malých tlakových vířivých trysek

**Stručná charakteristika problematiky úkolu:**

Tlakové vířivé trysky (TVT) jsou používány v mnoha aplikacích, např. pro rozprašování paliv ve spalovacích motorech různých typů. Tato klasická koncepce podléhá i v současnosti inovacím pro zvýšení technické hodnoty motoru jako celku. Pomocí optických měřících metod bude na několika TVT provedeno měření velikosti a rychlosti kapek ve spreji, průtočných charakteristik, stability spreje a dalších důležitých parametrů.

**Cíle diplomové práce:**

Hodnocení nestabilit spreje s využitím signálu tlakových pulzací v přívodní větvi trysky, případně jinou metodou
Mikroskopické pozorování výrobních nepřesností a posouzení vlivu na funkčnost trysky
Příprava a nastavení optického měřícího systému
Studium vlastností spreje několika variant TVT pomocí optických metod
Fyzikální analýza výsledků (posouzení struktury a geometrie spreje, korelace velikosti kapek s bezrozměrnými kritérii procesu), grafická prezentace výsledků.

**Seznam literatury:**

Bayel, L., Orzechowski, Z., Liquid atomization, Taylor & Francis, Washington, D.C., 1993

Khavkin, Y., The Theory and Practice of Swirl Atomizers, Taylor & Francis, 2004 - Počet stran: 462

ZHANG, Zh., LDA Application Methods: Laser Doppler Anemometry for Fluid Dynamics (Experimental Fluid Mechanics), Springer, ISBN: 9783642135132, 2010.

Dantec dynamics A/S. LDA and PDA Reference Manual. Tonsbakken 18, DK-2740 Skovlunde, Denmark, 2011

DANTEC DYNAMICS A/S. BSA Flow Software v5.00: User's Guide. Tonsbakken 18, DK-2740 Skovlunde, Denmark, 2010.

Lefebvre, A. H., and Ballal, D. R., 2010, "Gas turbine combustion alternative fuels and emissions," Taylor & Francis,, Boca Raton, pp. 1 online resource (xix, 537 p.).

Termín odevzdání diplomové práce je stanoven časovým plánem akademického roku 2015/16

V Brně, dne

L. S.

| | |
|---|---|
| doc. Ing. Jiří Pospíšil, Ph.D.<br>ředitel ústavu | doc. Ing. Jaroslav Katolický, Ph.D.<br>děkan fakulty |

## Summary

The present master thesis deals with an experimental study of spray characteristics from several small pressure-swirl atomizers used in a combustion chamber of turbojet aircraft engine. For decades, attention has been paid to improvement of their atomization characteristics but still there are possibilities which have not been examined yet. Investigations were carried out using various geometries of the individual elements of atomizer to find their effect on the spray. Measurements were made using a different number of entry ports (2, 3 and 4), various swirl chamber shapes (hemispheric; conical; curved convex and flat conical), and different spill-line orifice designs (axial and off-axial). Emphasis was placed on the assessment of spray stability wherein the fluctuating spray negatively affects the operating characteristics of the combustion chamber. Spray characteristics were probed using Phase Doppler analyser, spray circumferential homogeneity was rated by mechanical patternator and the liquid breakup was imaged by simple laser shadowgraph.



## Key words

Atomizer, pressure-swirl, spill-return, spray, droplet, breakup, Phase Doppler anemometry, patternator



## Abstrakt

Diplomová práce se zabývá experimentální studií vlastností spreje z několika malých tlakových vířivých trysek používaných ve spalovacích komorách proudových motorů. Po desetiletí byla snaha zlepšit jejich rozprašovací charakteristiky a stále jsou možnosti, které nebyly téměř prozkoumány. Výzkum byl proveden za použití různých geometrií jednotlivých dílů trysky za účelem zjištění jejich vlivu na sprej. Byl použit různý počet vstupních portů (2, 3 a 4), různé vířivé komůrky (kulová, kuželová, konvexní, nízká kuželová) a rozdílné návrhy obtokového otvoru (osové, mimosové). Důraz byl kladen na posouzení stability spreje, kde pulzující sprej negativně ovlivňuje provozní charakteristiky spalovací komory. Vlastnosti spreje byly proměřeny fázovým dopplerovským analyzátorem, cirkulární homogenita byla hodnocena mechanickým paternátorem a rozpad kapaliny byl vizualizován pomocí jednoduchého laserového stínografu.



## Klíčová slova

Atomizér, tryska, tlaková vířivá, obtok, sprej, kapka, rozpad, fázový dopplerovský analyzátor, paternátor

## Bibliographic citation

MALÝ, M. *Experimentální studie vlastností spreje a funkčnosti malých tlakových vířivých trysek.* Brno: Vysoké učení technické v Brně, Fakulta strojního inženýrství, 2016. 84 s. Vedoucí diplomové práce doc. Ing. Jan Jedelský, Ph.D.

## Affirmation

I declare that this master's thesis is the result of my own work led by doc. Ing. Jan Jedelský, Ph.D. and all used sources are duly listed in the bibliography.

Bc. Milan Malý

# Acknowledgments

Foremost, I would like to express my sincere gratitude to my supervisor doc. Ing. Jan Jedelský Ph.D. for his patience, motivation, enthusiasm and immense knowledge.

I am also grateful that I had the opportunity to work with equipment provided for research and scientific activities of NETME Centre, regional R&D centre built with the financial support from the Operational Programme Research and Development for Innovations within the project NETME Centre (New Technologies for Mechanical Engineering), Reg. No. CZ.1.05/2.1.00/01.0002 and, in the follow-up sustainability stage, supported through NETME CENTRE PLUS (LO1202) by financial means from the Ministry of Education, Youth and Sports under the „National Sustainability Programme I“. This work has been also supported by the project No. GA15-09040S funded by the Czech Science Foundation.

I would like to express my thanks to Ph.D. student Ing. Matouš Zaremba who give me some valuable advices and comments, to Lada Janáčková who helped me with the preparation of measurement. My gratitude also belongs to Dr. Graham Wigley for technical consultations and help with the Phase Doppler analyser.

Last but not least, I would like to thank my beloved girlfriend Jana for her encouragement and patience during writing this thesis and to family for the support they have provided me throughout my entire life.

# Contents

1 Introduction ..... 15
2 Spray development ..... 17
2.1 Liquid stream breakup ..... 17
2.1.1 Liquid sheet disintegration ..... 18
2.2 Droplets formation ..... 20
2.3 Droplets coalescence ..... 21
3 Pressure-swirl atomizers ..... 23
3.1 Atomizers with spill-line ..... 23
3.2 Atomizer parameters ..... 23
3.2.1 Discharge coefficient ..... 24
3.2.2 Sauter mean diameter ..... 24
3.2.3 Spray cone angle ..... 25
4 Experimental methods ..... 27
4.1 Test rig ..... 27
4.1.1 Instrumentation ..... 27
4.2 Laser anemometry ..... 28
4.2.1 Basic principles of Laser Doppler Anemometry ..... 28
4.2.2 Phase Doppler Anemometry ..... 29
4.2.3 PDA setup ..... 29
4.3 Shadowgraphy ..... 31
4.4 High speed imagining ..... 32
4.5 Mechanical patternation ..... 32
4.6 Spray fluctuation sensing ..... 33
4.6.1 Subjective evaluation of the spray fluctuations ..... 34
5 Tested atomizers ..... 35
6 Results and discussion ..... 37
6.1 Discharge parameters ..... 37
6.2 Subjective correlation ..... 40
6.3 Influence of the atomizer design on the spray characteristics ..... 42
6.3.1 Influence of the swirl chamber geometry ..... 43
6.3.2 Influence of the tangential ports number ..... 45
6.3.3 Influence of the spill-line orifice geometry ..... 47
6.4 Correlation of ISMD on Reynolds number ..... 53
6.5 Quality of manufacture and fault conditions ..... 54

6.5.1 Dimensional evaluation ..... 54
6.5.2 Surface damage ..... 55
6.5.3 Fault conditions ..... 56
7 Conclusion ..... 59
Bibliography ..... 61
List of symbols ..... 65
A. Conference paper at HydroTermo 2015 ..... 67
B. Conference paper at EFM 2015 ..... 71
C. Conference paper at AEaNMiFME 2016 ..... 79

# 1 Introduction

An atomization is a process of liquid disintegration into small fragments - drops. A flow of atomized liquid is called “spray” and it is generated in a spraying device - atomizer. This conversion is essential for many industrial applications such as combustion, water cooling, spray coating or food processing. Atomization can by carried out by variety of forces: mechanical, aerodynamic or ultrasonic [1]. A design of the atomizer depends on its application and operating conditions. The most common type are pressure atomizers due to their simple design. The simplest atomizer type is a plain orifice type whereas pressure-swirl type is more frequently used and it can be divided into several variations as simplex, dual orifice or spill-return. Unlike to the twin-fluid atomizers, no additional medium or energy is required.

In recent time, three theses dealing with sprays and atomization were written at Brno University of Technology. The work by Matouš Zaremba [2] deals with an influence of an operating condition on a twin fluid atomizer (effervescent type). Lukáš Durdina in [3] made a comparison of optical measuring methods on a spray generated by the pressure-swirl (PS) atomizer together with an extensive description of the liquid break up. The last thesis written by Milan Malý [4] analysed a performance of the pressure-swirl atomizer in terms of liquid properties at various inlet pressure. Principles, which have been evaluated in appointed theses, will not be discussed in detail.

This thesis is a sequel of author’s previous work [4] and it is focused on the pressure-swirl atomizers with various geometrical dimensions and its influence on spray quality and stability. In PS atomization, the internal flow structure is closely linked to the quality of the resulting spray. Any improvement in spraying performance leads to an increase of the combustion chamber efficiency and any fluctuations may harm the atomization as well as the combustion itself.

Figure 2-1, Figure 2-3 and Figure 6-7 were made in cooperation with Lada Janačková and they may be used also in her bachelor thesis.

# 2 Spray formation

In the following chapter, the spray development with focus on the pressure-swirl atomization will be discussed including primary and secondary breakup. The droplets coalescence will close this topic. Due to the complexity of whole spray generating process, only the fundaments will be presented.

## 2.1 Liquid stream breakup

Liquid breakup is a very chaotic and complex process. In order to understand the liquid disintegration principles, it is appropriate to begin with the simplest form of the liquid stream – plain jet. A liquid jet, see Figure 2-1, discharged into ambient air may breakup into the small droplets or ligaments when it is subjected to even minimal disturbances. These disturbances may be in form of a surface displacement, pressure fluctuation in a supply system as well as fluctuations in liquid properties such as temperature, viscosity or surface tension [5].

There are four important forces acting on the liquid in terms of atomization: Gravity force, viscous force, surface tension force and inertia. From these four forces, three dimensionless criteria may be defined [6]:

Reynolds number:
$$\mathrm{Re} = \frac{Inertia}{Viscous\ \ forces} = \frac{\rho_l \cdot D \cdot V}{\mu_l} \tag{1}$$

Weber number:
$$We = \frac{Inertia}{Surface\ tension\ \ forces} = \frac{\rho_l \cdot D \cdot V^2}{\sigma_l} \tag{2}$$

Ohnesorge number:
$$Oh = \frac{Viscous}{\sqrt{Inertia \times Surface\ \ tension\ \ forces}} = \frac{\sqrt{We}}{\mathrm{Re}} = \frac{\mu_l}{\sqrt{\sigma_l \rho_l D}} \tag{3}$$

where $D$ is a characteristic length and $V$ is a characteristic velocity. The liquid properties are represented by the liquid density $\rho_l$, liquid dynamic viscosity $\mu_l$ and surface tension $\sigma_l$. For some cases, the Froude and Bond number may be defined but these numbers are not evaluated in this thesis.

The dimensionless numbers for gas phase can be written in the same way: the gas-phase Reynolds number and the gas-phase Weber number where the fluid properties correspond to properties of the surrounding air.

The first study of the instability of liquid jets was presented by Rayleigh [7] in 1878. He obtained an equation for droplets grow rate using an assumption of an inviscid liquid flow. Rayleigh mechanism (similar to the droplet formation in Figure 2-1) is applicable at low Oh and Re where the aerodynamic interaction with surrounding air is neglectable. With increasing liquid velocity, the liquid breakup occurs closer to the atomizer's exit orifice and the droplets become smaller. The whole mathematical solution based on the Navier-Stokes equations and the continuity equation is reviewed in [5, 6] and it is beyond the scope of this thesis.

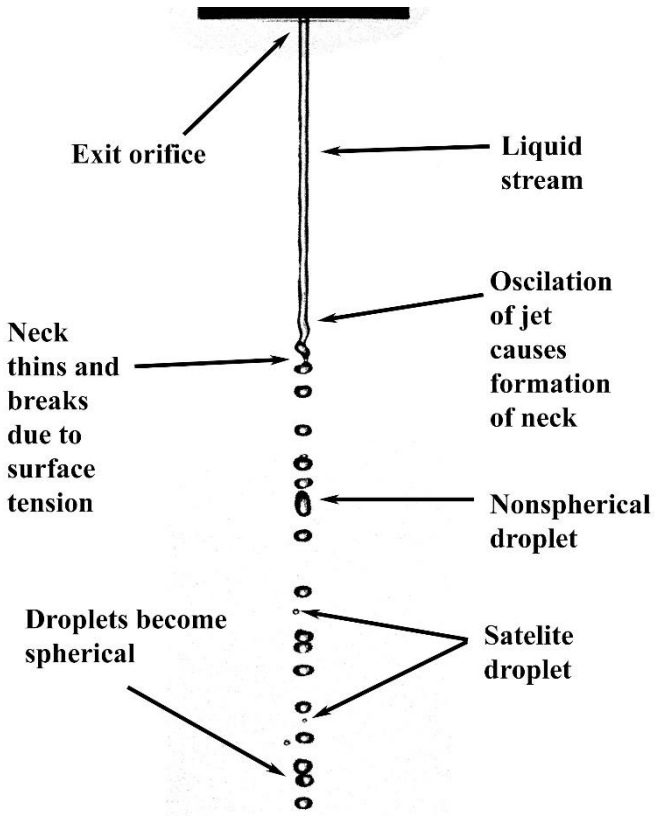


***Figure 2-1*** *Droplet formation of low velocity liquid stream*

### 2.1.1 Liquid sheet disintegration

In many atomizers, including the pressure swirl type, the bulk liquid is transformed into thin liquid sheet which is subsequently atomized due to interaction between discharged liquid and surrounding air. The liquid sheet disintegrates into smaller objects called filaments in terms of primary breakup while in the secondary breakup are these filaments broken into small droplets [1], as it is shown in Figure 2-2. The droplet size is generally in the same order of thickness as the liquid sheet thickness [5]. The liquid sheet breakup is described in detail by Lin et al in [8]. Besides the extensive mathematical description of the liquid jet and sheet instabilities they summarize general findings which are affecting the liquid sheet stability. They found that the rate of disturbance decrease as Re and We are decreased. This implies that the inertia force relative to viscous and surface force causes the destabilization of the liquid sheet.

As it was mentioned above, the liquid sheet formation depends on Re and We which are functions of the liquid inertia. The liquid inertia depends on the liquid velocity which is related to the inlet pressure. At very low inlet pressure the liquid sheet is not formed (see Figure 2-3) and the PS atomizer behave like a plain jet atomizer and the atomization is driven by the Rayleigh mechanism. When the inlet pressure increases, the liquid sheet begins to occur. This stage (according to Lefebvre [1]) is called an onion stage. When the pressure difference grows, the spray shape changes to a tulip stage (at 0.15 MPa in case of atomizer in Figure 2-3) with wider spray cone. From this stage the liquid sheet may be considered as developed. With further pressure grow, the cone is slightly wider while the breakup length decreases rapidly in accordance to high Re and We which cause a strong disturbance in the liquid sheet.

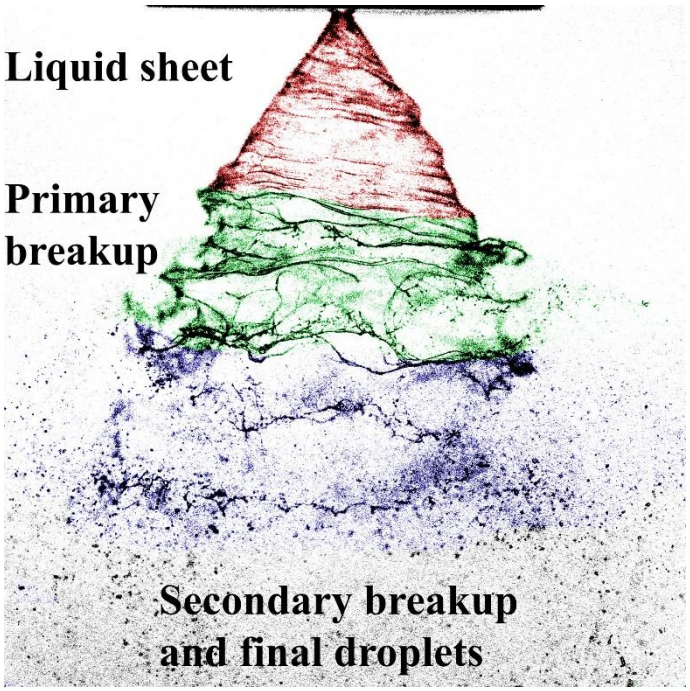


***Figure 2-2*** *Liquid sheet disintegration, kerosene 0.5 MPa*

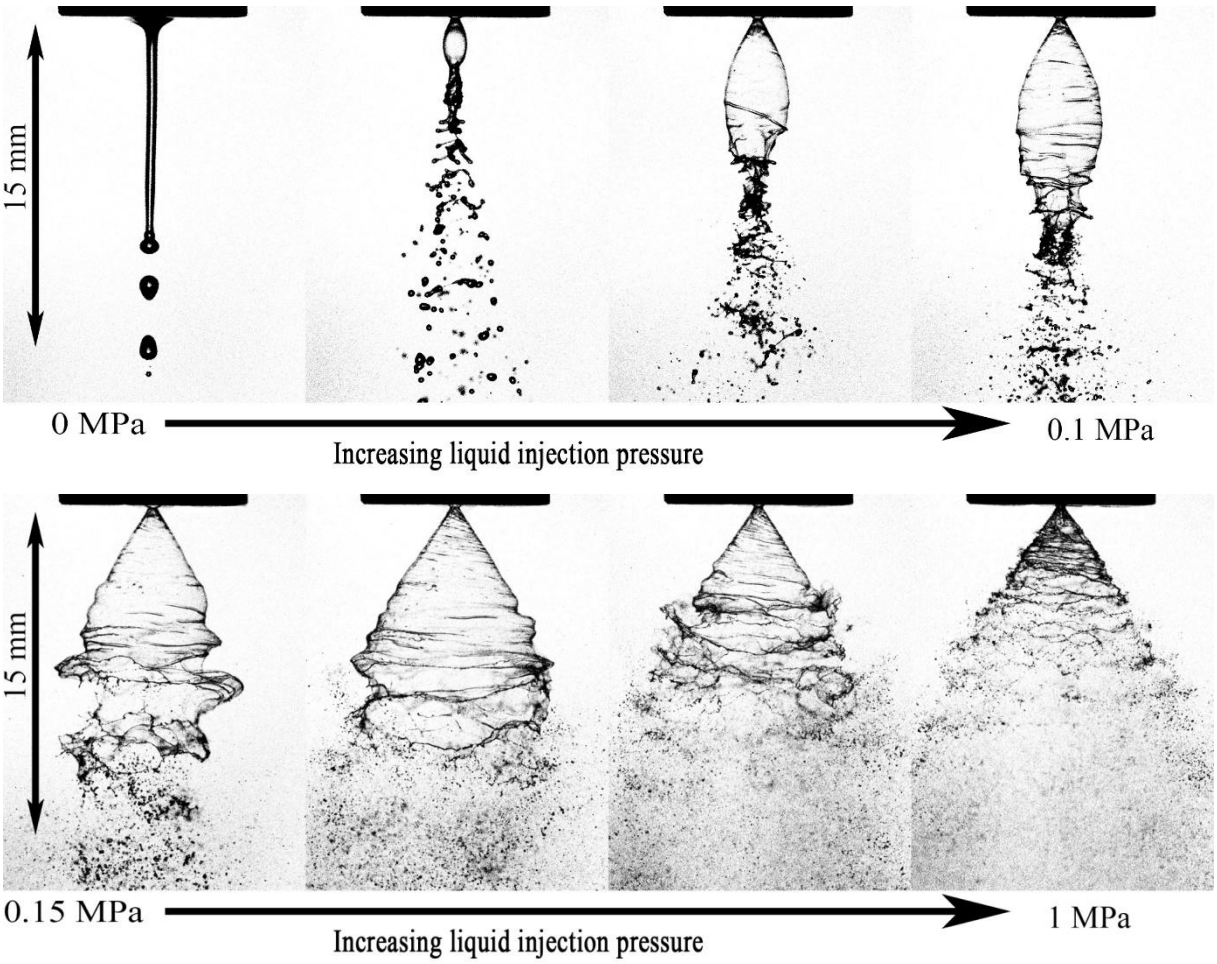


***Figure 2-3*** *Liquid sheet formation as a function of liquid inlet pressure, simplex atomizer using kerosene*

## 2.2 Droplets formation

When the liquid sheet disintegrates breakup into ligaments and large droplets in the primary, the atomization process is not finish yet. In the secondary breakup are these ligaments subjected to surrounding atmosphere, moving with relative velocity, the aerodynamics forces may cause Its deformation and break apart into fragments. This phenomena was recently review by Guildenbecher in [9] and he described the process of secondary breakup as:

*"The process starts when the drop enters the disruptive flow field. This marks the beginning of the deformation phase. An unequal pressure distribution, due to acceleration of the ambient fluid around the drop, leads to deformation from the initial spherical shape. This deformation is resisted by the interfacial tension and viscous forces. However, if the aerodynamic forces are large enough the drop will enter the fragmentation phase."*

Depending on the flow regime (We number), the breakup may occur as vibrational, bag, multimode, sheet-thinning and catastrophic. The flow with the lowest We breaks, due to droplet oscillations, as vibrational into a few fragments of similar size. With an increasing velocity the We number grows and the bag breakup happens. The drop is flattened and subsequently blown out in the direction of flowing air, creating thin hollow bag and thicker toroidal rim. Thin bag disintegrates into large number of small droplets whereas the rim generates small number of large fragments. The multi-mode breakup appears when the We number exceeds approximately We = 35 and it is similar to the bag breakup. The difference is in the addition of a stamen in the centre of the drop. Like the bag breakup, the bag is atomized followed by the rim at first and the stamen which results in multi-size fragments. With a high relative velocity, the sheet-thinning and the catastrophic breakup mode occurs. In the first case is the drop surface continuously eroded creating a large amount of small droplets. The remaining drop core may be (in some cases) in the same order of magnitude as the original droplet. In the catastrophic breakup, the drop disintegrates rapidly into small drops which may break up into even smaller ones. This process is beard by the surface waves and the drop break in the whole volume.

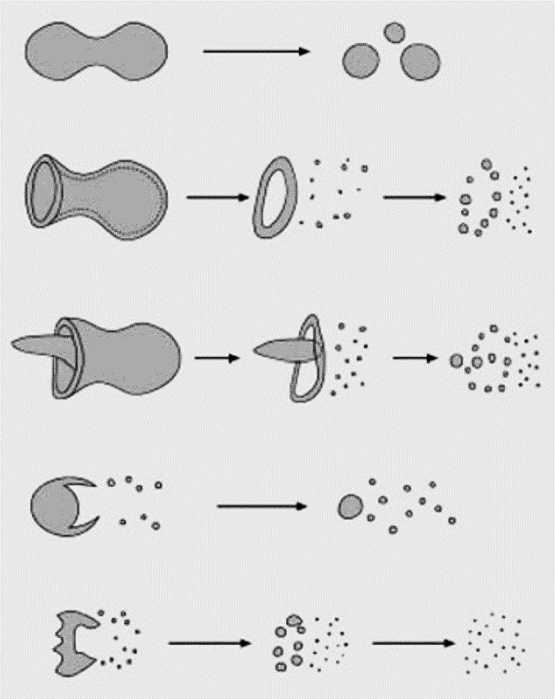

- Vibrational
  - $0 < We < 11$
- Bag
  - $11 < We < 35$
- Multi-mode
  - $35 < We < 80$
- Sheet-thinning
  - $80 < We < 350$
- Catastrophic
  - $We > 350$

***Figure 2-4*** *Newtonian drop breakup morphology, valid for Oh < 0.1. Adapted from [9]*

The temporal evolution of the secondary breakup is illustrated in Figure 2-5 (adapted from Schmehl [10]). The non-dimension time (X axis) is defined as a ratio of time and the characteristic deformation time $t^*$:

$$t^* = \sqrt{\frac{\rho_l}{\rho_g}} \frac{D_0}{V} \tag{4}$$

For all breakup modes is common that the drop flattens during an initial phase. The breakup starts when $t/t^* = 2\text{-}3$ and ends at $t/t^* = 4\text{-}7$ depending on the breakup mode. Between the start and the end is a phase of various sub processes which determine a formation of liquid structures.

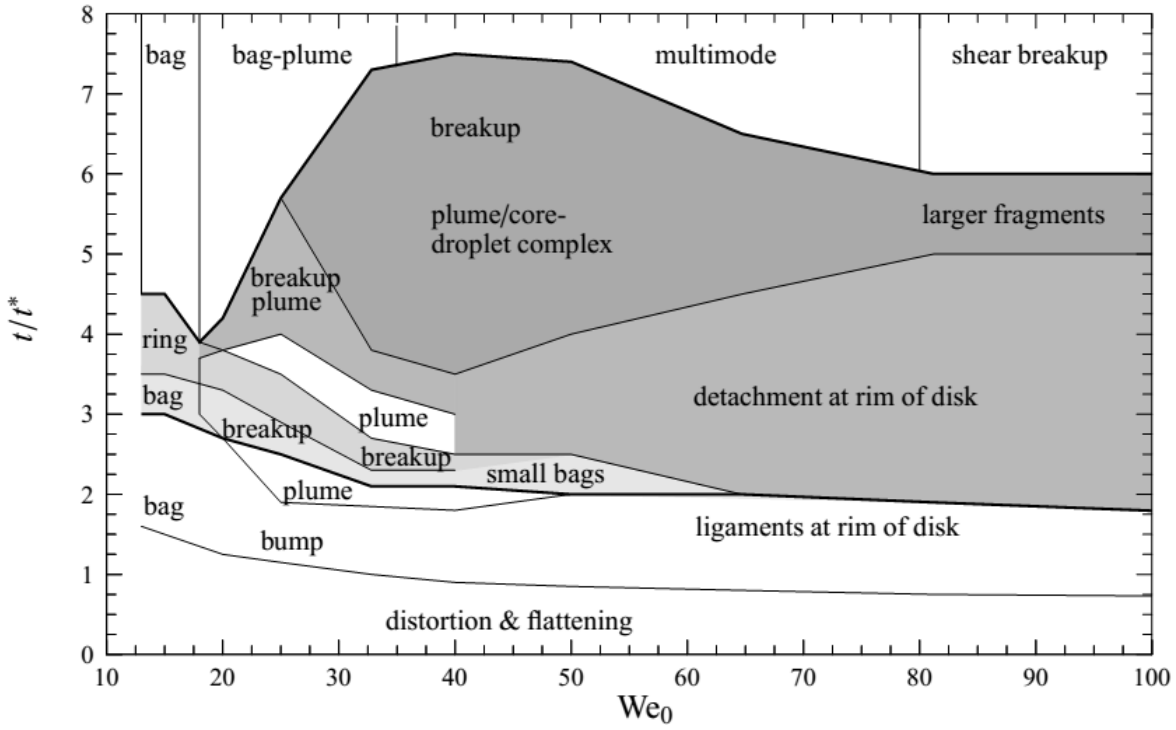


***Figure 2-5*** *Temporal evolution of droplet breakup, Oh < 0.1. Adapted from [10]*

## 2.3 Droplets coalescence

After the drops formation, the dense nature of the droplet concentration is formed thus the droplet collision is expected to be a frequent event and may significantly modify the subsequent spray development and combustion characteristics [11]. Figure 2-6 schematically shows the possible regimes of the droplet collisions where the *B* is the impact parameter defined for the same sized drops as:

$$B = \frac{\chi}{2R} \tag{5}$$

where the *R* is droplet radius and $\chi$ is the separation distance between the droplet centres. The We number takes into account the relative velocity between interacting droplets.

One of the basic collision regimes is a coalescence emerging at low relative velocity and small separation distance. When the separation distance is increased, drops will bounce each

other. When increasing the We, transient regimes of bouncing droplets will occur as well. However, this regime is absent for water droplets thus the (a) and (c) merge [11]. At the high We a separation regimes are creating an extra satellite droplet.

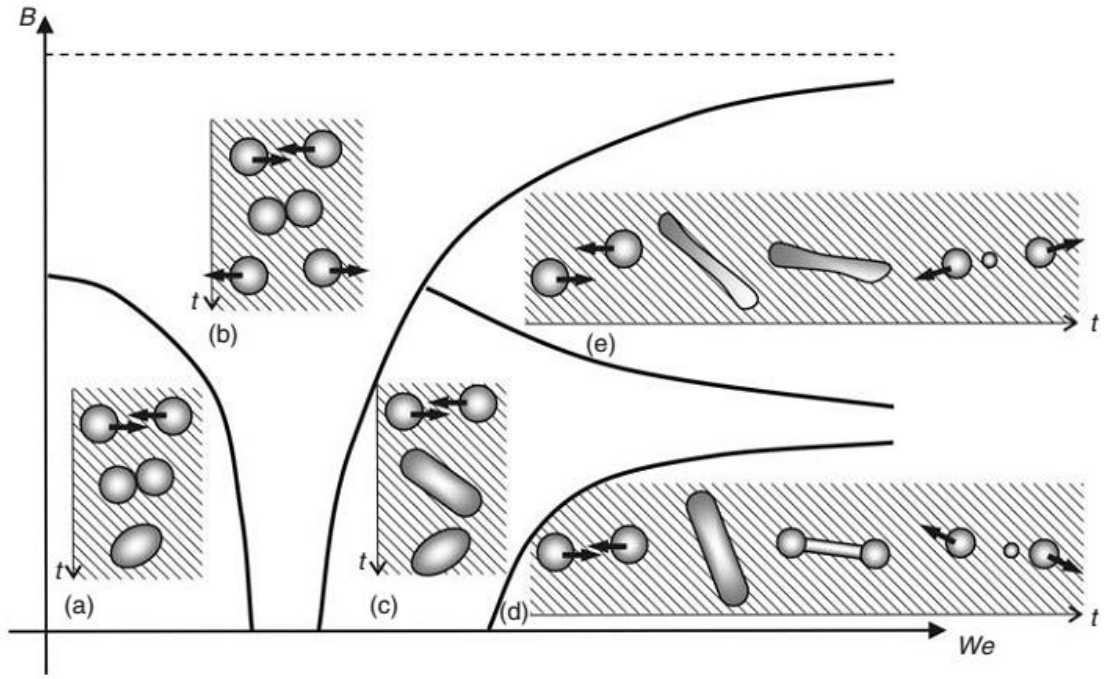


***Figure 2-6*** *Collision regimes for the same sized hydrocarbon droplets: a) coalescence; (b) bouncing; (c) coalescence; (d) reflexive separation; (e) stretching separation. Adapted from [12]*

# 3 Pressure-swirl atomizers

Pressure swirl atomizers are used for more than one century in combustion systems, water cooling systems and in many other industrial applications. Compared to other atomizers, their main advantages are construction simplicity, high atomizing efficiency and high reliability. A drawback may be a wide dispersion of droplet sizes.

The basic pressure-swirl atomizer is a simplex type (simplex due to simplicity of its design). It consists of three parts: inlet tangential ports, a swirl chamber and an exit orifice. The liquid is injected via the tangential ports into the swirl chamber, gaining swirl motion under which the liquid leaves the exit orifice and spreads as a conical liquid film outside the atomizer. These atomizers have a disadvantage in a fact, that the droplet size is proportional to the inlet pressure hence to the liquid mass flow rate. This drawback is solved using the pressure swirl atomizers with the spill-line or the dual orifice atomizers [13].

## 3.1 Atomizers with spill-line

The pressure-swirl atomizer with a spill-line (often called spill-return type) is basically the simplex type which consist a passage in the rear wall of the swirl chamber. The liquid, injected via tangential ports, is divided into two streams; one of them is discharged outside and atomized while the second one is "spilled" back to the reservoir through the spill-line (SL) orifice. Main advantage of this system is that the fuel is always supplied to the swirl chamber at the high pressure providing good atomization over a wide span of the injection flow rate. It is redeemed by demands of a powerful pump. If the exact amount of the injected liquid must be known, there must be two flow-meters in the fuel supply– one in the feeding line and the second in the spill line.

## 3.2 Atomizer parameters

The atomizer geometry as well as the liquid properties plays a significant role in the quality of atomization, affecting the liquid mass flow rate, the liquid sheet thickness, the cone angle etc.

The pressure swirl atomizer with the spill-line is schematically drawn in Figure 3-1. The functional dimensions are listed in Table 3-1 and influence some of them on the discharge characteristics and spray quality will be discussed later in this thesis based on the

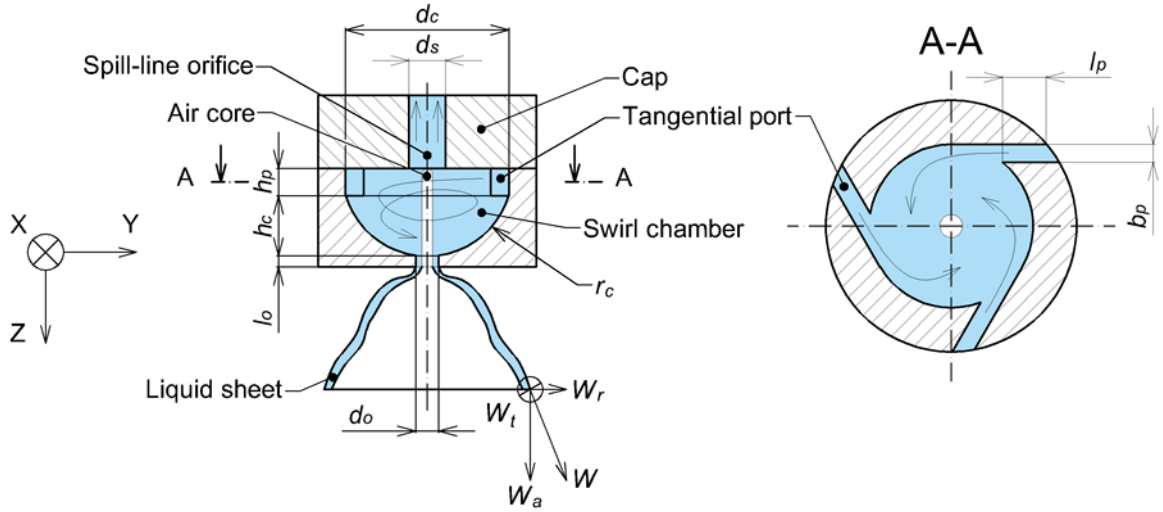


***Figure 3-1*** *Schematic drawing of the pressure swirl atomizer with the spill-line*

experimental results.

***Table 3-1*** *Atomizer characteristics dimensions in millimetres*

| Nomenclature | Description |
|---|---|
| $l_p$ | Length of the inlet tangential port |
| $l_o$ | Length of the exit orifice |
| $b_p$ | Width of the inlet tangential port |
| $h_p$ | Height of the inlet tangential port |
| $h_c$ | Height of the swirl chamber |
| $d_c$ | Width/diameter of the swirl chamber |
| $d_s$ | Diameter of the spill-line orifice |
| $d_o$ | Diameter of the exit orifice |
| $r_c$ | Radius of the swirl chamber* |

* If the swirl chamber is not spherical, determining dimension will be e.g. bevel

### 3.2.1 Discharge coefficient

Coefficient of discharge ($C_D$) is a ratio between the actual and the theoretical mass flow rate through the exit orifice, defined as:

$$C_D = \frac{\dot{m}_l}{\dot{m}_{teor}} = \frac{\dot{m}_l}{A_o \sqrt{2\rho_l \Delta p}} \tag{6}$$

where $A_o$ is area of the exit orifice. The $C_D$ is for pressure swirl atomizers usually low due to the presence of the air core blocking off the central portion of the exit orifice and it is roughly independent on the inlet pressure. Rizk and Lefebvre in [14] derived equation in terms of atomizer dimension as:

$$C_D = 0.35\left(\frac{A_p}{d_s d_o}\right)^{0.5}\left(\frac{d_s}{d_o}\right)^{0.25} \tag{7}$$

where $A_p$ is total area of tangetial ports: $A_p = n \cdot b_p \cdot h_p$

### 3.2.2 Sauter mean diameter

Sauter mean diameter (SMD, $D_{32}$) is often used in applications where the surface area plays significant role such as combustion (it is the vapour that burns) or drying etc. It is roughly a ratio of the droplet volume to its surface area:

$$SMD = D_{32} = \frac{\sum_{i=1}^{n} n_i D_i^3}{\sum_{i=1}^{n} n_i D_i^2} \tag{8}$$

where $D_i$ is diameter of the particle (measured) and $n_i$ is number of measured particles.

In non-uniform sprays, it is necessary to define a single parameter to characterize a global spray quality (especially when point-to-point measuring method is used). The integral Sauter mean diameter (ISMD) fits well to that task [15]:

$$ISMD = ID_{32} = \frac{\sum_{i=1}^{n} r_i f_i D_{30,i}^3}{\sum_{i=1}^{n} r_i f_i D_{20,i}^2} \quad (9)$$

where $r_i$ is radial distance of measured point to the spray centre, $f_i$ is data rate at measured point, $D_{30,i}$ is volume mean and $D_{20,i}$ is surface mean diameter.

The smallest possible SMD is usually required in combustion applications providing large surface area to the small volume which is good for evaporation and subsequently for combustion itself. In previous work [4] was made an extensive review of factors affecting SMD:

- SMD decreases rapidly with increasing liquid pressure
- Increasing liquid viscosity and surface tension lead the increase of SMD significantly
- High density liquid and dense surrounding air have positive effect on SMD. This effect is not significant due to small disparity of these values in practice
- Smaller atomizers – with lower flow rate produce smaller droplets
- Wider spray cone reduces SMD

### 3.2.3 Spray cone angle

An important aspect of the atomizer design is the spray cone angle (SCA). In general, an increase in the SCA leads to a greater exposure of the droplets to the surrounding air which may result in improved atomization, may affect ignition performance, flame blowout limits and pollutant emission [1]. SCA may be estimated in dependence on the liquid properties and the atomizer dimensions by an empirical correlation [16]:

$$2SCA = 16.2\left(\frac{A_p}{d_s d_o}\right)^{-0,39} d_o^{1,13} \mu_l^{-0,9} \Delta p^{0.39} \quad (10)$$

# 4 Experimental methods

Experiments were performed on a special designed facility for cold spray testing under controlled conditions on Brno University of Technology.

## 4.1 Test rig

The tested liquid (fuel) was supplied to the atomizer by a special designed fuel supply track (Schematic layout in Figure 4-1). The liquid, stored in the fuel tank (1), is pumped) via filter (2) by a gear pump (3) to the atomizer (9). The liquid mass flow rate is regulated by driving the pump speed and fine regulation is reached by needle valve (13) in the pump spill-line. The amount of pumped fuel is measured in the inlet line by a Coriolis mass flow meter (4). Liquid overpressure is measured by a piezo-resistive sensor (7) and pressure fluctuations are measured by a piezo-electric sensor (8) close to the atomizer (9). The inlet line is also equipped by a temperature reading. The spill-line is equipped by a static pressure meter (10), ball valve (11) and positive displacement flow meter (12). Atomized liquid is collected by the collection chamber and flows back into the fuel tank. Fuel mist and vapours were ventilated by a fan.

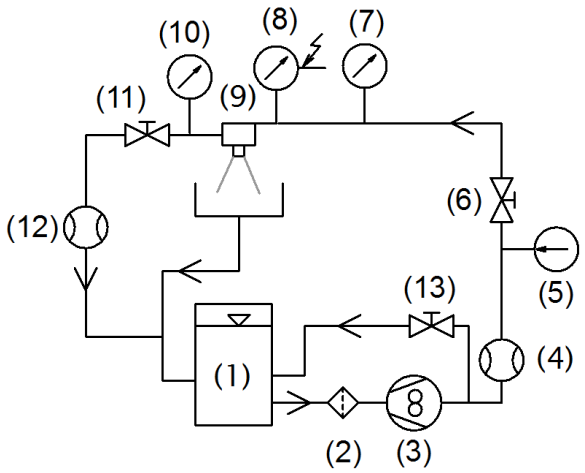


***Figure 4-1*** *Fuel supply*

### 4.1.1 Instrumentation

The flow rate in the inlet line was measured by Siemens Mass 2100 Di3 Coriolis mass flow meter fitted with a Mass 6000 transmitter. At flow rates above 12.5 kg/h the accuracy declared by manufacturer was ±0.1 % of the actual flow rate. For the flow rates below 12.5 kg/h the error could be calculated using the formula:

$$E = \pm\sqrt{0.01 + \frac{1}{\dot{m}_l}} \tag{11}$$

where E is the error of the flow meter in [%] and $\dot{m}_l$ is the actual flow rate [kg/h]. The liquid density can be also measured with this device with an error of $\pm 1.5\ \mathrm{kg/m^3}$ from the measured value.

In the spill-line, the liquid volume flow rate was measured by the positive displacement flow meter Kobold with the accuracy 1% of actual reading. The volume flow reading was consequently recalculated to the mass flow rate using the liquid density measured by the Coriolis mass flow meter.

The resistance temperature detector (RTD) Omega PR-13 was mounted in the fuel line. An operating range of -30 to 350 °C and an accuracy of $\pm$ 0.2 °C of the actual temperature was declared by the manufacturer.

Pressure was measured with two BD Sensors DMP 331i with a range of 0-17 bar and the error declared by the manufacturer is to be less than $\pm$0.35 % of the actual pressure [4].

The fast response piezo-electric pressure sensor is described in chapter 4.6.

## 4.2 Laser anemometry

Due to an inability to properly predict or simulate the atomization process, measurement taken on the real atomizers have its indispensable role. Among the important parameters measured in sprays belongs particle velocities in all directions and a particle size which is used to calculations of representative diameters e.g.: SMD and ISMD. Phase Doppler anemometry (PDA) serves this purpose well with time-resolved measurement of the particle velocities and size. The principles of this technique are explained in detail in several monographies [17-19] and were also closely elaborated by Matouš Zaremba in [2].

### 4.2.1 Basic principles of Laser Doppler Anemometry

Laser Doppler anemometers (LDA) are non-contact optical instruments for measuring the velocity of gases, liquids and solids. This apparatus consists, in the simplest form, from a high power laser, several lenses, photo-detectors and processing device. The special properties of usable laser are the spatial and temporal coherence. At all cross sections along the laser beam, the intensity has to have a Gaussian distribution. When two coherent monochromatic laser beams intersect at given angle $\Theta_b$, they will interfere and create fringe pattern – parallel lighter and darker planes as shown in Figure 4-2. The distance between fringes $\delta_f$ depends on the laser wavelength and the angle between the incident beams [20]:

$$\delta_f = \frac{\lambda}{2Sin\frac{\theta_b}{2}} \tag{12}$$

A particle crossing normal to the fringes with velocity U produces refract light and generates a signal with a sinusoidal oscillation frequency of $f_d$:

$$U = \delta_f f_d \tag{13}$$

The primary result of a laser anemometer measurement is a current pulse from the photo-detector. This current signal contains the frequency information related to the velocity to be measured [20].

In order to determine the direction of the particle movement, one of the interacting beams is shifted by a shift frequency. In the fringe model this corresponds to a movement of the fringes. A particle moving with the fringes yields a lower frequency and movement against the fringes generate a higher frequency.

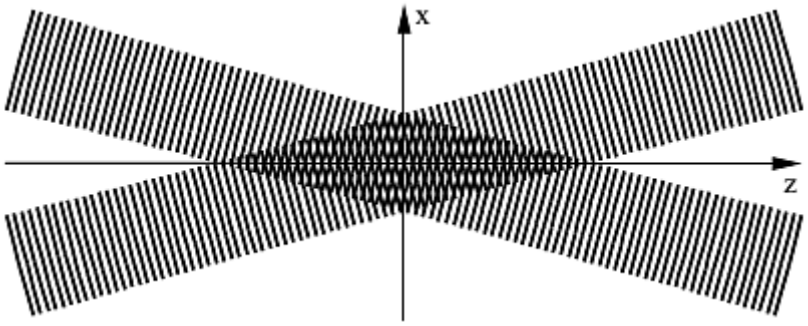


***Figure 4-2*** *Fringe pattern*

### 4.2.2 Phase Doppler Anemometry

The LDA is suitable for velocity measurement only. If the information about the particle size is required, the Phase Doppler Anemometry takes its place. Basically, it is an extension of the LDA with two or more photo-detectors. The optical path to the photo-detectors is different with the varying angular position of the detectors. When the particle passes through the measuring volume, both photo-detectors receive a Doppler burst of the same frequency but the phases of the signal is shifted. If all geometric parameters of the optics remain constant the signal shift depends only on the droplet size, as shown in Figure 4-3.

The two-detector system can distinguish only a phase shift between zero and $2\pi$. Therefore, if a particle has a size that causes the phase to go over $2\pi$, the system cannot determine between this size and a much smaller particle. This ambiguity can be overcome by an additional detector (receiving optics with three photo-detectors) [20].

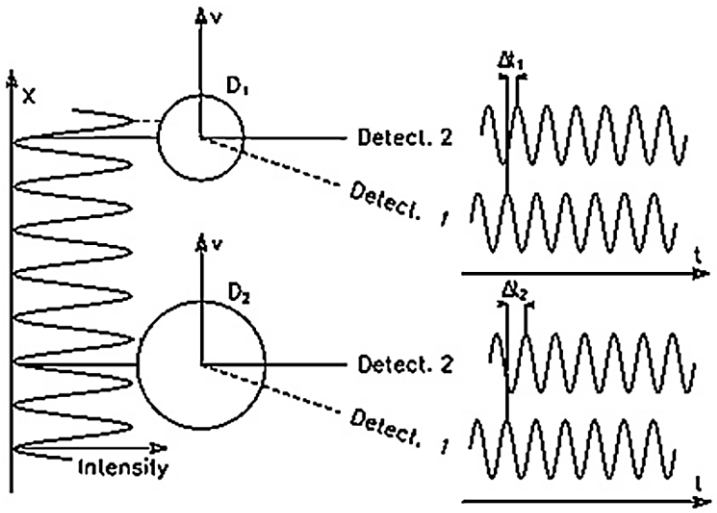


***Figure 4-3*** *Signal shift related to the droplet size, adapted from [20].*

### 4.2.3 PDA setup

Measurements were done with 2D fibre PDA made by Dantec Dynamic A/S. This system is schematically drawn in Figure 4-4 and it is composed of:

- Spectra physics Stabilite 2017 Argon laser with maximal power output of 6 W.
- 60X41 Transmitter box
- 60X81 2D 85 mm Transmitting optics beam expander

- 57X50 112 mm diameter fibre PDA receiver optics with spatial filter
- Fibre PDA Detector unit
- BSA P80 Flow and Particle Processor

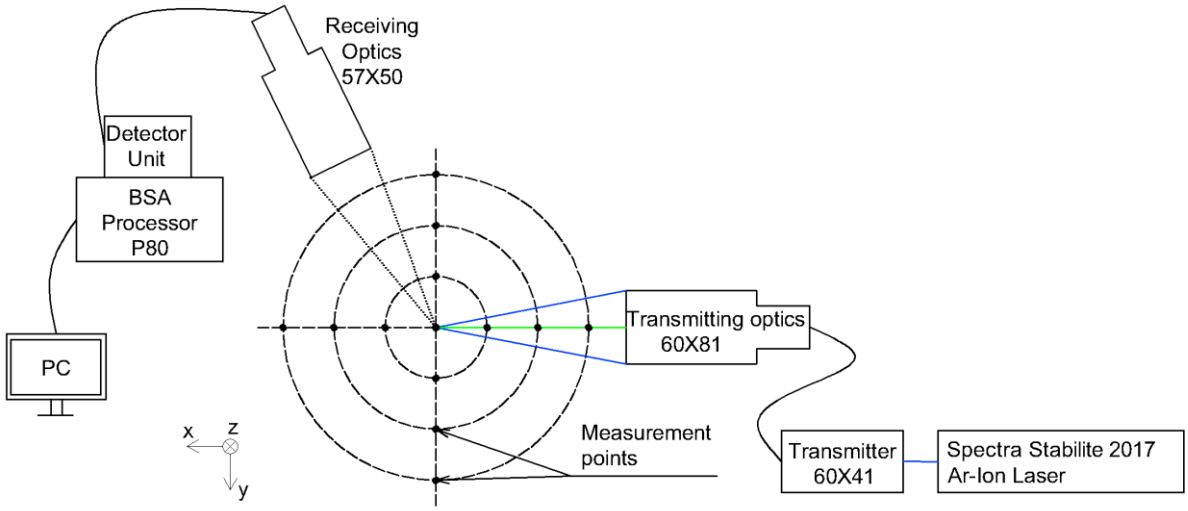


***Figure 4-4*** *PDA schematic layout*

During the last three years several tests were done in order to establish the proper system configuration in terms of the data-rate and validation rate. Parameters, which affect the system behaviour, are summarized together with values in this thesis in Table 4-1. The system setup is based on setup used in [4] but several improvements were done. Parameters which determine signal strength such as laser power, sensitivity, signal gain and signal to noise ratio (SNR) were thoroughly balanced using oscilloscope. Optics focal length together with the mask determines the maximal particle diameter. If the wrong combination is chosen, the smallest or greatest particle would not be detected or validated. The velocity center and span define the range of detectable particle velocities and it is set to detect every particle in the spray.

***Table 4-1*** *PDA setup*

| Parameter | Value |
|---|---|
| Laser power output | 0.5 W |
| Wavelength | 488 nm and 514.5 nm |
| Front focal length of transmitting optics | 310 mm |
| Front focal length of receiving optics | 800 mm |
| Scattering angle | 70° |
| Mask | B |
| Spatial filter | 0.050 mm |
| Maximal particle size | 165 μm |
| | |

| Velocity | Axial | Radial, Tangential |
|---|---|---|
| Velocity center | 18 m/s | 0 m/s |
| Velocity span | 48 m/s | 45 m/s |
| Sensitivity | 800 V | 1000 V |
| SNR | 0 dB | 3 dB |
| Signal gain | 20 dB | 20 dB |
| Level validation ratio | 8 | 2 |

## 4.3 Shadowgraphy

PDA data give us quantitative information about the spray characteristics but tells us nothing about the atomization process, breakup length or the spray instabilities (fluctuations of very unstable spray are detectable using PDA – see appendix A Conference paper at HydroTermo 2015 ). For this reason, it is convenient to have detailed image of the spray structure and breakup process. Because the liquid leaves the exit orifice under relatively high velocity and the atomization happened in a short distance, a very fast image exposition is required. Several cameras and light sources were tested during last two years reaching shutter speed below 1/20000 without significant success – see Figure 4-6a. These findings lead to search for a light source with an extreme short pulse and such light source was found in a particle image velocimetry (PIV) system. This system uses Nd:YAG high energy pulse laser with the pulse length of 5 ns (equivalent of camera shutter speed 1/20000000). After several modifications, very simple and effective method of the spray visualization was put together without any costly investment.

The new system is configured for taking backlight (shadow) photography - Figure 4-5. Laser beam from the Nd:YAG laser is first expanded by an eyepiece from a microscope and then is diffused by an opaque glass. The image is captured by a conventional DSLR camera with fitted macro lens. In this thesis was used Canon 70D with Canon 100 mm f/2.8 USM Macro. The only drawback of the classic camera is the impossibility of the precise time synchronization which has to be done by hand. Results compared to the conventional xenon flash (expose time about 50 μs) is in Figure 4-6. From this picture is evident that the xenon flash has very long expose time causing a motion blur over the whole picture even if the picture is captured from greater distance.

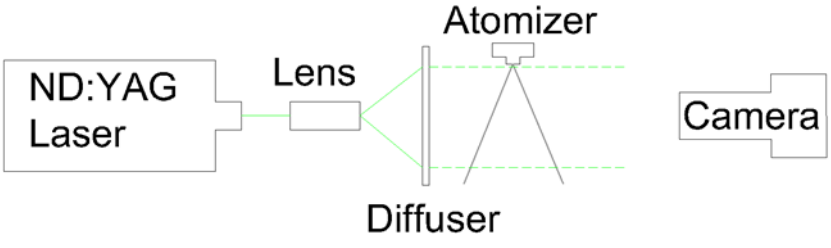


***Figure 4-5*** *Simplified scheme of the shadowgraph imagining system*

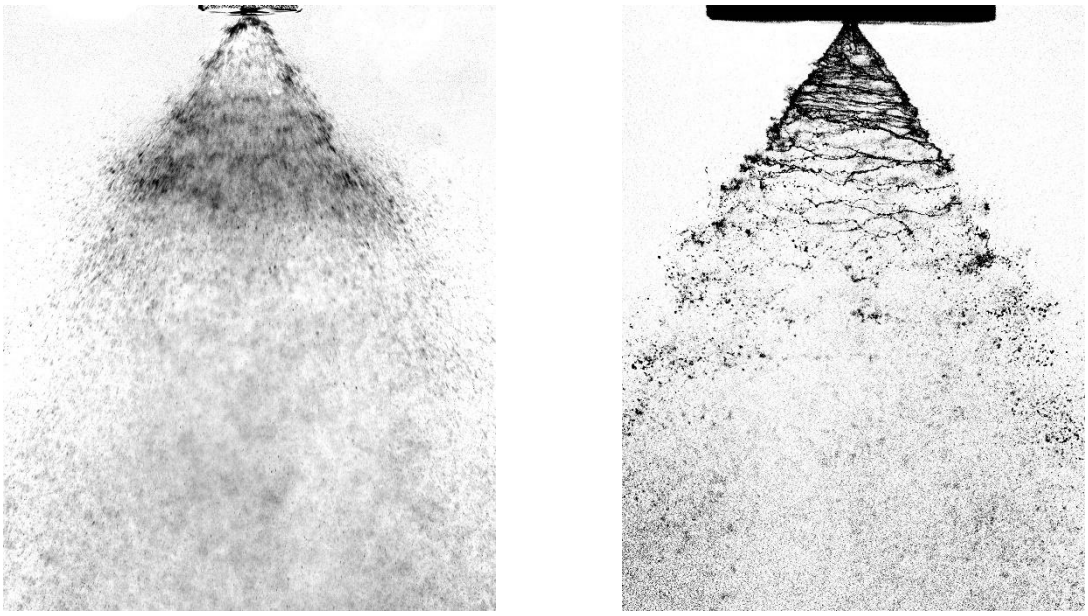

a) Xenon flash [4] b) Nd:YAG laser

***Figure 4-6*** *A comparison of xenon flash and Nd:YAG pulse laser, 1 MPa, kerosene*

## 4.4 High speed imagining

Beside the photography which produces a static picture in high resolution, it is often helpful to have time-resolved images of the liquid breakup and the spray itself. For this reason, high speed camera Photron Fastcam SA-Z 2100K was recently received. Together with home-built high power LED light it is possible to make a record with 100,000 frames per second (or faster) which is fast enough to capture time-resolved liquid breakup in detail.

## 4.5 Mechanical patternation

The symmetry of the spray patterns produced by the atomizer is an important parameter in many applications, e.g.: non-uniformities in circumferential fuel distribution in gas turbine combustors can lead to a rise of local pockets of low fuel-air mixture in which burning rates are low, thereby produce high concentrations of carbon monoxide and unburned hydrocarbons [21]. The liquid circumferential distribution was rated by a simple circular-sectored vessel called mechanical patternator with 16 pie-shaped sectors, as shown in Figure 4-7. The volume of each sector is 60 ml. The duration of each test is determined by the time required for one of the sectors to become nearly full, usually it is between two and three minutes. The height of the liquid from the upper edge in each sector was measured by a calliper. The values were consequently averaged to get mean height and the levels of the sectors were normalized against the mean height. The coefficient of variation was calculated as a single parameter describing the non-uniformities.

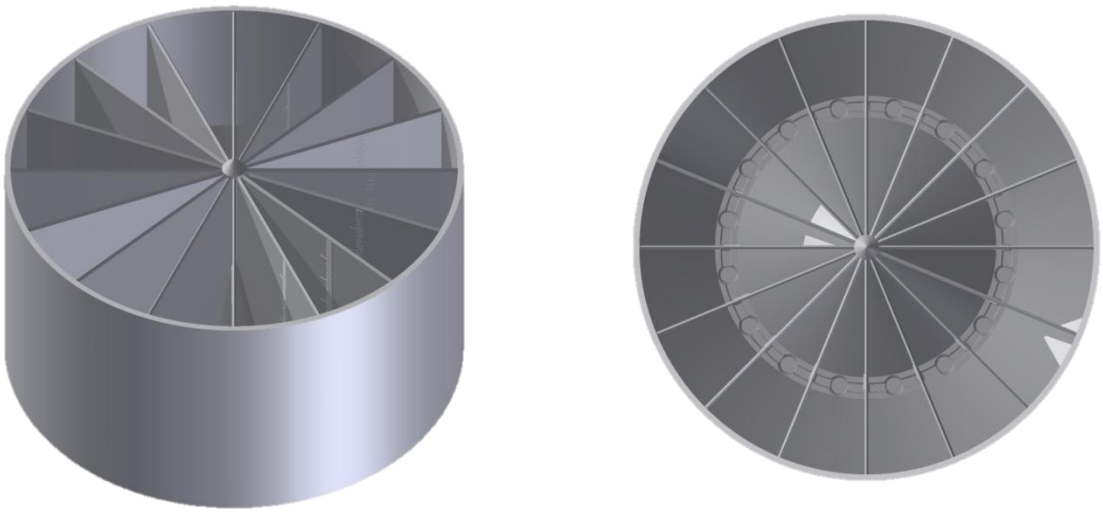

***Figure 4-7*** *Model of mechanical patternator*

## 4.6 Spray fluctuation sensing

The spray instabilities formed inside the swirl chamber may generate a feedback deeper into the liquid supply line which is detectable as a pressure fluctuation and can be measured by a rapid response pressure sensor. For this purpose, piezoelectric pressure sensor Kistler 701A was selected and the measurements were done at sampling rate of 1600 Hz. The time-resolved data were converted into a frequency domain using a Fast Fourier Transform (FFT) and subsequently categorized into the frequency windows (0-1 Hz, 1-25 Hz, 1-50 Hz and 0-800 Hz). Mean and median amplitudes were calculated as a single numerical value in each window in sake of different atomizers comparison one each other. In order to choose only one value as the representative, correlations with the subjective observation (see chapter 4.6.1) and discharge coefficient were done for all tested atomizers (40 different atomizers, in total 120 regimes). Coefficient of determination $R^2$ was calculated for each frequency group (see Table 4-2) as a parameter that indicate how the data fits the linear regression. From this analysis is evident that the median values prove better correlations with both parameters in almost each frequency group. Frequencies up to 1 Hz does not have a functional dependence possibly due to the presence of the pressure static component and still, they are much lower than the real spray fluctuating frequency. The highest correlation factors were achieved by the median in the range of 1-50 Hz and this parameter will be used in following evaluations. Moreover, the spray fluctuation rate was estimated by high speed visualization to frequencies between 3-20 Hz and it fits well to the group 1-50 Hz.

***Table 4-2*** *Coefficient of determination between pressure fluctuations and subjective observation resp. $C_D$*

| **Coefficient of determination with subjective observation** | | | | |
|---|---|---|---|---|
| | **0-1 Hz** | **1-25 Hz** | **1-50 Hz** | **0-800 Hz** |
| **Mean** | 0.00 | 0.41 | 0.41 | 0.30 |
| **Median** | 0.01 | 0.47 | 0.49 | 0.45 |
| **Coefficient of determination with discharge coefficient** | | | | |
| | **0-1 Hz** | **1-25 Hz** | **1-50 Hz** | **0-800 Hz** |
| **Mean** | 0.03 | 0.28 | 0.38 | 0.25 |
| **Median** | 0.03 | 0.29 | 0.41 | 0.15 |

### 4.6.1 Subjective evaluation of the spray fluctuations

The subjective observation was focused on the spray fluctuations in order to determine the impact of the pulsations on the spray cone. It was based (as name suggested) on the subjective perception of changes in the spray cone angle and assessed according to the scale in Table 4-3. The results helped to find an empiric description of the spray fluctuations.

***Table 4-3*** *Scale of subjective evaluation*

| Scale | Description |
|---|---|
| **1 - 2** | Stable |
| **3 - 4** | Weak fluctuations, small effect on the spray cone angle |
| **4 - 6** | Medium fluctuations |
| **7 - 10** | Strong fluctuation |

# 5 Tested atomizers

More than 40 different atomizers were tested in order to achieve a stable spray and find the effects of the atomizers dimensions on the spray characteristics. Chosen variants, which were subjected to PDA measurements, are shown in Figure 5-1 and their dimensions are listed in

Table 5-1 and Table 5-2. The dimension's aberrations are in agreement with chapter 3.2.

Four swirl chambers are varying in the design of the convergent part. Used shapes are: A - hemispheric, B - conical; C - curved convex and D - flat conical.

Six caps differ in the position of the SL orifices. Among tested variants belong: Simplex – SS, axially-positioned - S1; axially-positioned with low height of the inlet ports – S1LP, off-axis spill orifices with the orifice axes: parallel - S2; radially-inclined toward the main atomizer axis - S3 and tangential to the flow - S4.

The T2, T3 and T4 are simplex caps with variable number of the tangential entree with constant total flow cross-section of the ports.

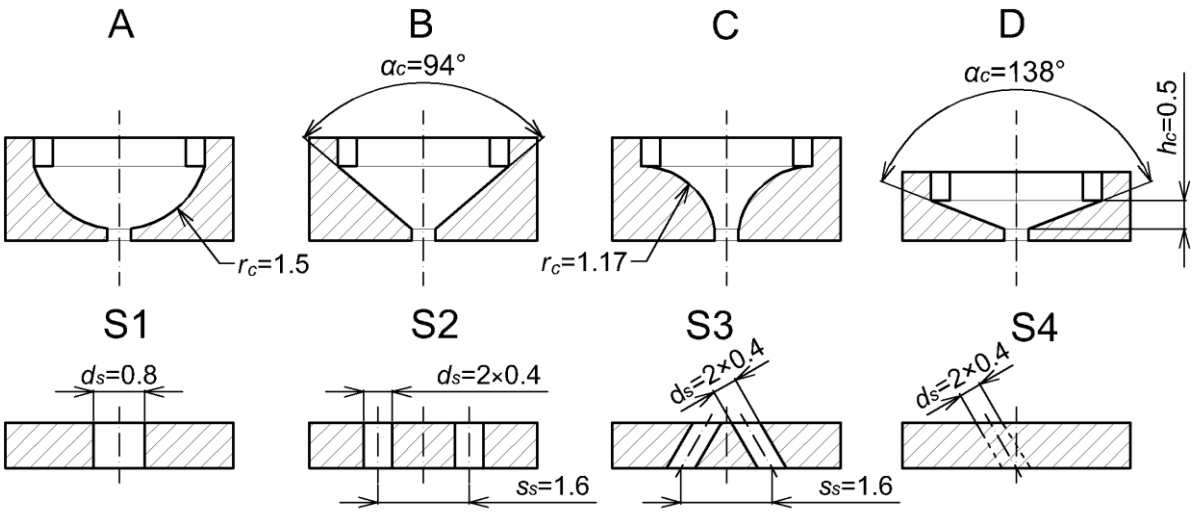


***Figure 5-1*** *Schematic representation of main tested variants*

***Table 5-1*** *Dimensions of the swirl chambers*

| Type | $d_o$ | $d_s$ | $h_s$ |
|---|---|---|---|
| [-] | [mm] | [mm] | [mm] |
| **A** | 0.42 | 3 | 1.1 |
| **B** | 0.42 | 3 | 1.1 |
| **C** | 0.42 | 3 | 1.1 |
| **D** | 0.42 | 3 | 0.5 |
| **AL*** | 0.45 | 3 | 1.1 |

*The same design as the A chamber

***Table 5-2** Dimensions of the caps*

| Type | No. of ports | $h_p$ | $b_p$ | No. of SL orifices | $d_l$ |
|---|---|---|---|---|---|
| [-] | [-] | [mm] | [mm] | [-] | [mm] |
| **S1** | 2 | 0.8 | 0.4 | 1 | 0.8 |
| **S1LP** | 2 | 0.35 | 0.9 | 1 | 0.8 |
| **S2** | 2 | 0.6 | 0.6 | 2 | 0.4 |
| **S3** | 2 | 0.6 | 0.6 | 2 | 0.4 |
| **S4** | 2 | 0.6 | 0.6 | 2 | 0.4 |
| **SS** | 2 | 0.6 | 0.6 | Simplex | - |
| **T2** | 2 | 0.5 | 0.5 | Simplex | - |
| **T3** | 3 | 0.5 | 0.33 | Simplex | - |
| **T4** | 4 | 0.5 | 0.25 | Simplex | - |

The atomizers with an obstacle which blocks off direct axial flow throught the axially placed SL orifice were tested in Conference paper at EFM 2015 and they are excluted from results in this thesis.

Kerosene jet A-1 was used as tested liquid. The physical properties of jet A-1 at room temperature (20 °C) were: $\sigma = 0.029$ kg/s$^2$, $\mu_l = 0.0016$ kg/(m·s), $\rho_l = 795$ kg/m$^3$. All PDA tests were done with one batch at 20 °C.

# 6 Results and discussion

In this chapter, the results from PDA measurement, discharge parameters and manufacturing quality will be presented and discussed.

Some results were processed into articles which were presented on scientific conferences. The effects of spill-line orifice geometry on the spray was dealt in Conference paper at HydroTermo 2015 and Conference paper at EFM 2015 (see in the appendix A and B). The influence of the liquid properties was experimentally studied in Conference paper at AEaNMiFME 2016 (see in the appendix C). Those particular results are not discussed in this chapter.

## 6.1 Discharge parameters

Pressure-dependent atomizer characteristics such as the mass flow rate, the discharge coefficient and the pressure fluctuations in the inlet line were investigated in detail using stable, partially-stable and unstable atomizer. The results are summarized in Figure 6-1, Figure 6-2 and Figure 6-3 respective. The atomizers were measured in a pressure range from 0.2 to 1.6 MPa in step of 0.1 MPa. The liquid breakup was visualized in three pressure regimes for each atomizer – see Figure 6-4.

The stable atomizer (D-SS) has the stable spray in every regime and the fully developed inner flow is likewise anticipated. The mass flow rate is characterized by an exponential curve where the increment of the flow rate is decreasing with increasing inlet pressure because the pressure loss in the atomizer increases as the square of the flow rate.

The discharge coefficient calculated by eq. 6 is slightly depended on the inlet pressure varying from 0.47 at lowest pressure to 0.44 at the highest tested pressure and fits well ($R^2 = 0.99$) with a power function as $C_D \propto \Delta p^{-0.039}$. $C_D$ was, beside the direct measurement of the flow rate, calculated using eq. 7 that is based only on the atomizer dimensions and results in $C_D = 0.43$ (dashed line) which is lower value than measured. However, the difference is neglect able at high inlet pressure. The similar descending slope was reported by Lan [22], Rashid [23] and Couto [24] whereas Ballester [16] observed nearly constant $C_D$, however his measurement were done for the inlet pressure above 1 MPa. Regarding to the inviscid theory, the $C_D$ should be constant and independent on the pressure. In our case we have to take into account real viscous flow where the liquid mass flow rate is related to the air core diameter - larger air core is blocking off the larger portion of the exit orifice which results in to a lower value of $C_D$. An increase in the liquid pressure is accompanied by an increase in the swirl velocity inside the swirl chamber. This cause an increase in the air core size. This conclusion was confirmed by Datta [25] in a numerical simulation of the internal flow inside the pressure-swirl atomizer.

In the stable spray, the pressure fluctuations are up to 1 Pa/MPa without any dependency on the inlet pressure. The liquid breakup corresponds to the idea of PS atomization. The liquid sheet is discharged from the atomizer and it is consequently braked up into the ligaments and droplets - see Figure 6-4.

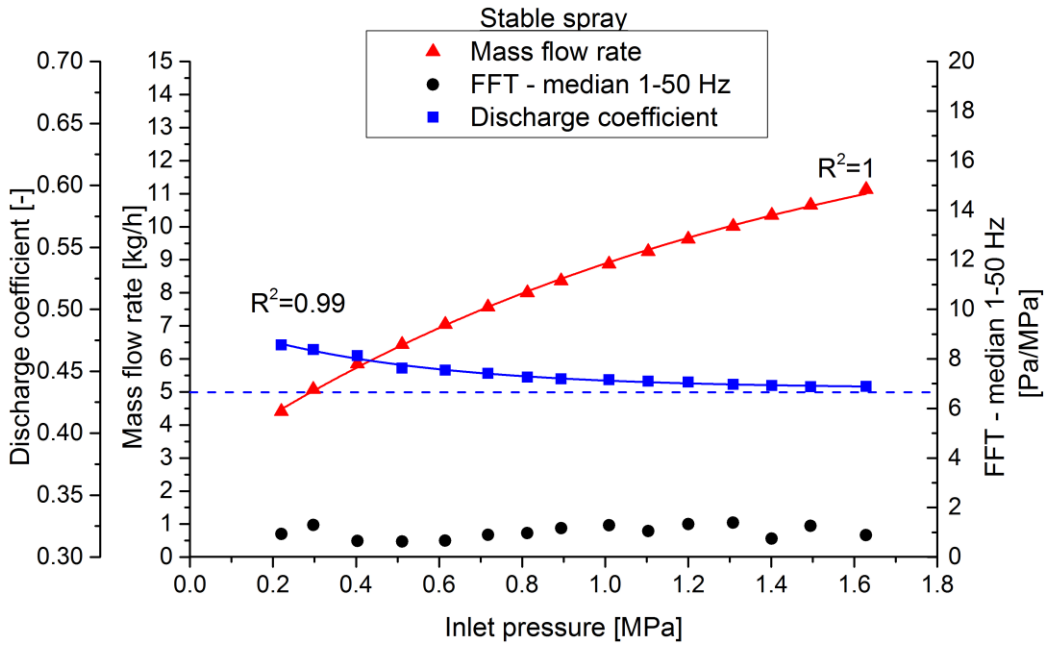


***Figure 6-1*** *Mass flow rate and $C_D$ related to the inlet pressure, the stable atomizer*

An identical evaluation process was done for the partially stable (D-S1LP) and the unstable atomizer (D-S1). The partially stable atomizer is shown in Figure 6-2. Until the pressure raises up to 0.9 MPa, the spray is visually unstable but the fluctuations disappear when the pressure is increased above 0.9 MPa. ¨Compared to the stable spray (Figure 6-1), the $C_D$ (and the mass flow rate as well) is much higher in the unstable regime and despite to the optical stability of the spray is the $C_D$ at the maximal pressure about 25 % greater than is it theoretical value. The pressure fluctuations are in the unstable region in rage of 2 - 4 Pa/MPa. In the stable regime is the maximum 1 Pa/MPa and it corresponds to the stable atomizer from Figure 6-1. In the unstable regime, the liquid breakup happened chaotically without generating liquid sheet. In the stable regimes are distinguishable fragments of the liquid sheet, however there are greater disturbances than in the case of the stable atomizer D-SS.

The unstable atomizer has very high $C_D$, differing about 35 % from its theoretical value at the highest pressure and it is even higher at lower pressure. The correlation coefficient of an exponential fit ($R^2$ = 0.91) is worse than in the stable sprays indicating to more chaotic inner flow. The pressure fluctuations show uniformity with varying inlet pressure reaching maximum of 8 Pa/MPa at 1.2 MPa and minimum of 1.5 Pa/MPa at 0.3 MPa. This behaviour may indicate a dependence of the spray pulsations on the inlet pressure and brings some level of uncertainty to determination of the spray fluctuation rate based on the inlet pressure pulsation. From the visual (Figure 6-4) point of view, the liquid breakup happened chaotically without any signs of the liquid sheet.

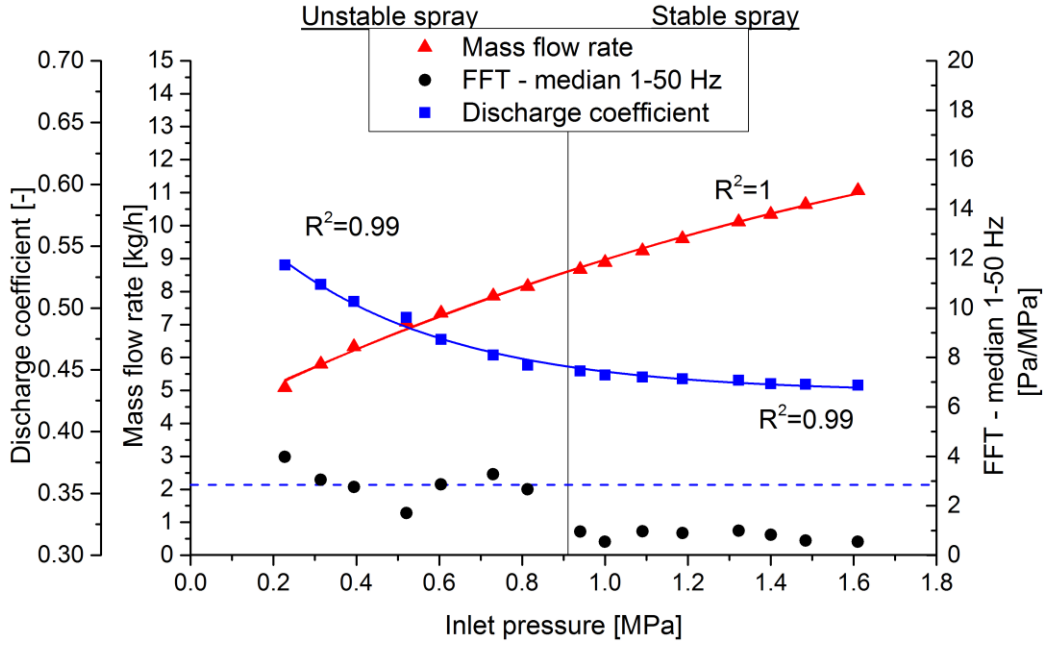


***Figure 6-2*** *Mass flow rate and $C_D$ related to the inlet pressure, the partially stable atomizer*

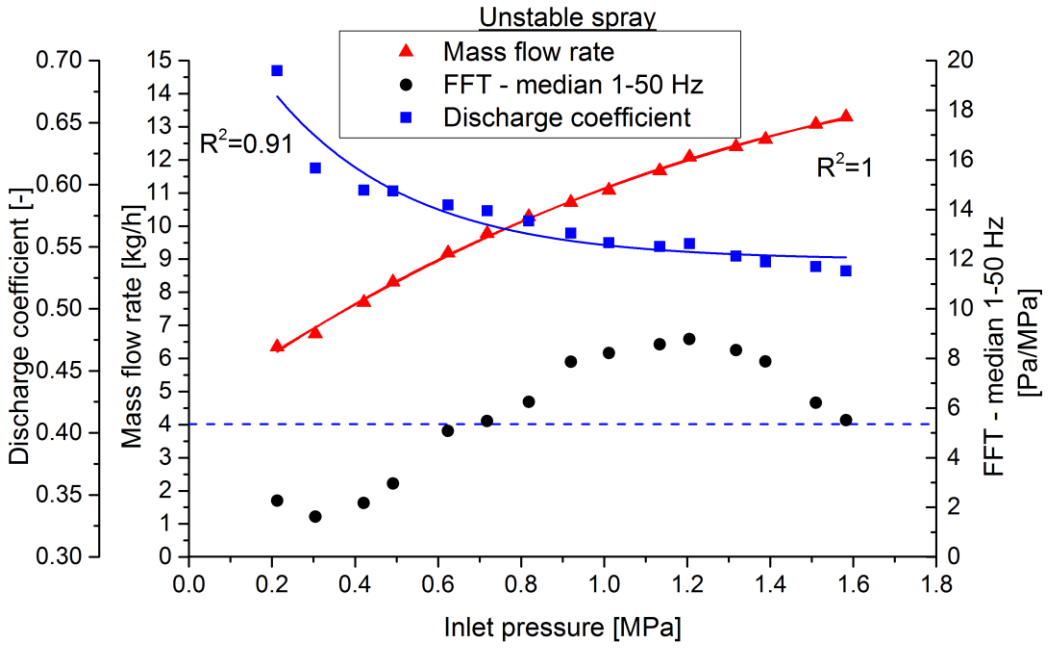


***Figure 6-3*** *Mass flow rate and $C_D$ related to the inlet pressure, the unstable atomizer*

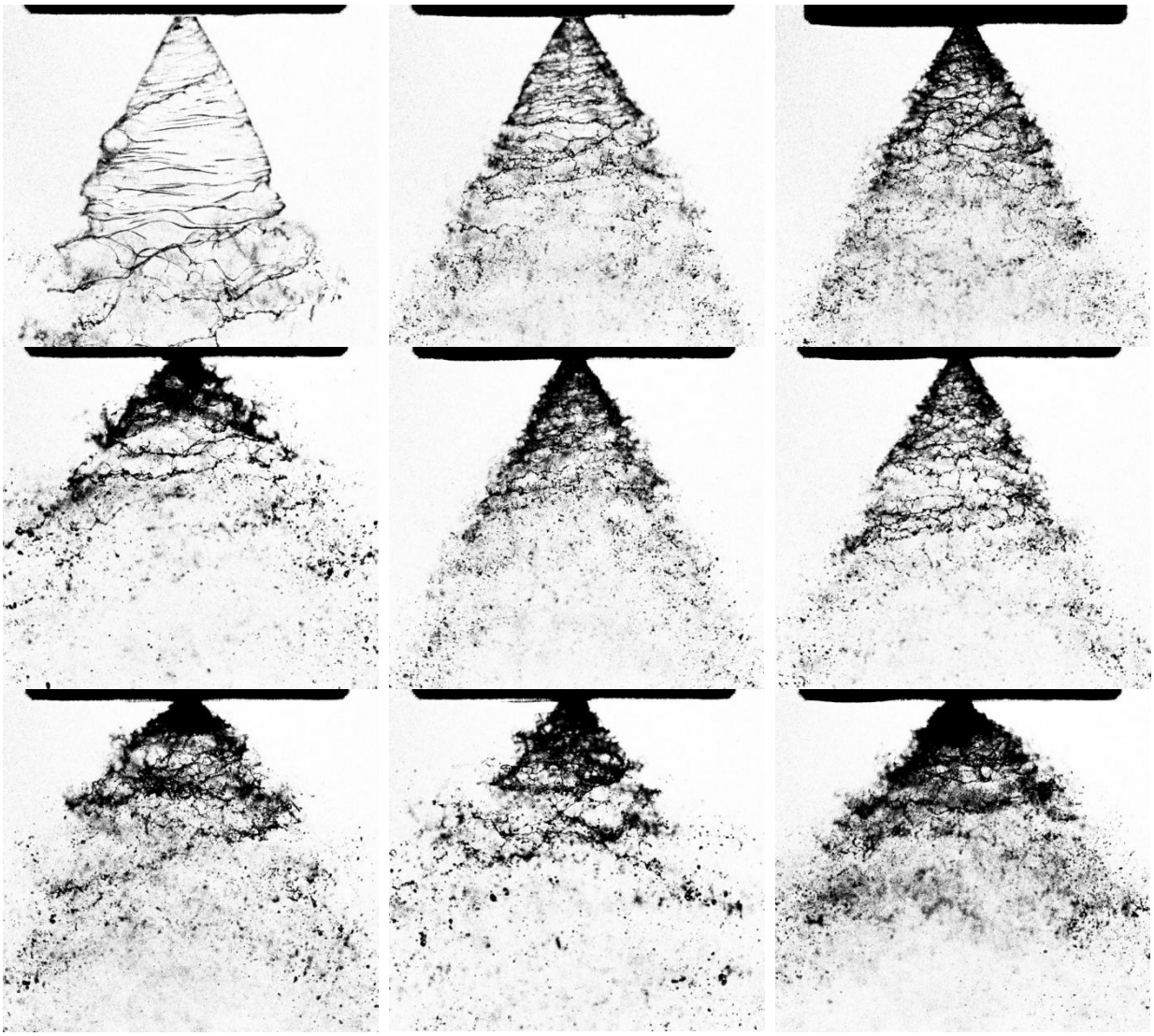

***Figure 6-4*** *Spray structure. From top: Stable, partially stable and unstable atomizer. From left: 0.5, 1 and 1.5 MPa*

The origin of the higher $C_D$ and greater pressure fluctuations is related to the inner air core which extends through the SL orifice hence is stretched and starts to behave unstable. The stretched air core disappears until it is reconstructed by the swirling liquid. Without the air core is the flow cross-section of the exit orifice larger thus the mass flow rate is higher (see Appendix B.: Conference paper at EFM 2015 ). As the consequence of the inner fluctuations we can detect pressure pulsations in the inlet line. These pulsations also disturb the generated liquid sheet which is practically undetectable and the liquid breakup happened very close to the exit orifice.

## 6.2 Subjective correlation

Based on the findings from the chapter 6.1, a correlation between the $C_D$, pressure fluctuations and the subjective observation may be determined in the order to establish an empirical evaluation method of the unstable sprays. Forty atomizers, tested in three regimes each (0.5, 1 and 1.5 MPa with closed SL), are plotted in Figure 6-5 in dependence on a relative discharge coefficient and the pressure-weighted median of pressure fluctuations in the group of 1-50 Hz. The relative discharge coefficient is defined as the measured $C_D$ (eq. 6) divided by the theoretical $C_D$ (eq. 7) and determine an amount of increase in the $C_D$

(respective an increase in the mass flow rate) compared to an ideal atomizer. Subjective observation is represented by a colour scale.

For sake of simplicity, the number of varying parameters was reduced by choosing only one swirl chamber thus the diameter of exit orifice and the shape of the swirl chamber itself remain constant. The result is presented in Figure 6-6. Similar evaluations were done for other single atomizers parts. It was found that the spill-line orifice geometry had very strong effect on the spray stability while the influence of the swirl chamber and the exit orifice dimensions was found as insignificant. Due to that, the atomizers were divided by the SL orifice into three categories in the plots for clarity.

The simplex atomizers have the $C_D$ very close to the theoretical one. Their relative $C_D$ is varying from 1 to 1.05. All simplex atomizers were stable and measured pressure fluctuations are up to 2.5 Pa/MPa. Similar results were obtained for the atomizers with the off-axis spill-line orifices. These geometries were stable but the relative $C_D$ becomes higher (up to 1.3) in some cases. The atomizers with the co-axis SL orifice were both, stable and unstable, with predominance of the unstable types, reaching very high relative $C_D$ (1.7) and high pressure fluctuations (17 Pa/MPa).

In a global perspective it is not possible to establish a generally valid correlation between the pressure fluctuations and the relative $C_D$ because the coefficient of determining is small ($R^2 = 0.36$). Nevertheless, it is possible to set borderlines delimiting the unstable atomizers. The relative $C_D$ higher than 1.35 or the pressure fluctuations above 2.5 Pa/MPa ensures an unstable atomizer.

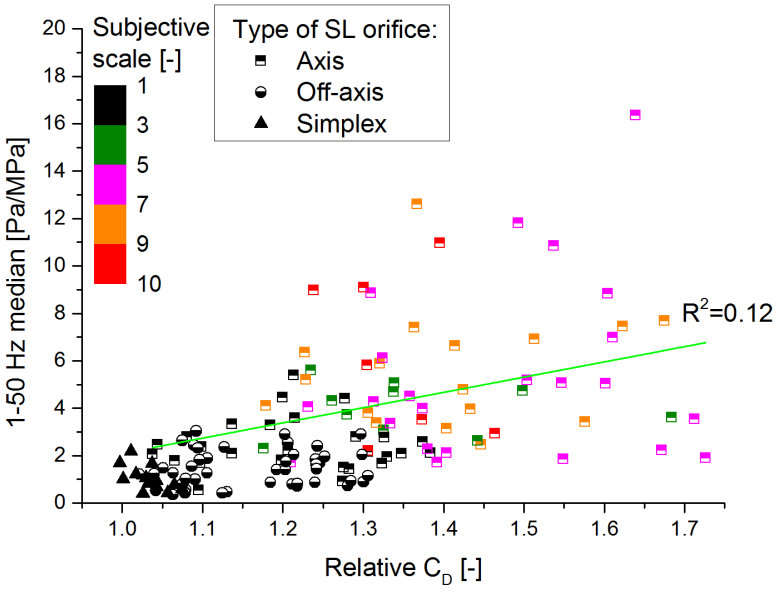


***Figure 6-5*** *Correlation of relative $C_D$ with pressure fluctuations*

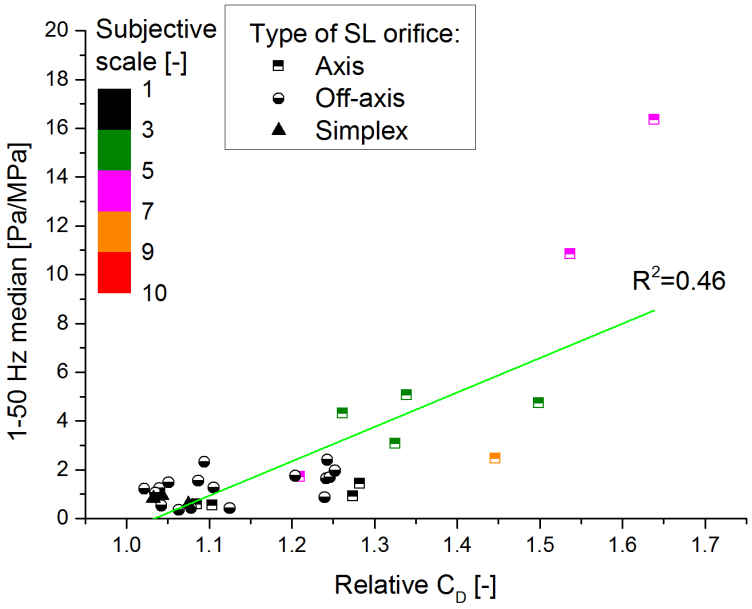


***Figure 6-6*** *Correlation of relative $C_D$ with pressure fluctuations for atomizers with equal swirl chamber*

Because of the prediction uncertainty of the spray fluctuation using the pressure sensor and $C_{D,}$ it is appropriate to find an alternative method for the detection of the spray pulsation. The spray cone fluctuations may be captured using the imaging system or by the high speed imagining. From the resulting images is calculated root mean square (RMS) image where the brightness of each pixel represents the rate of changes among whole image series in that particular point. RMS image can be used to determine the degree of the spray cone deviation – see Figure 6-7 where the cone deviations are highlighted by the red lines. However, due to processing complexity of this method it was not used in this thesis.

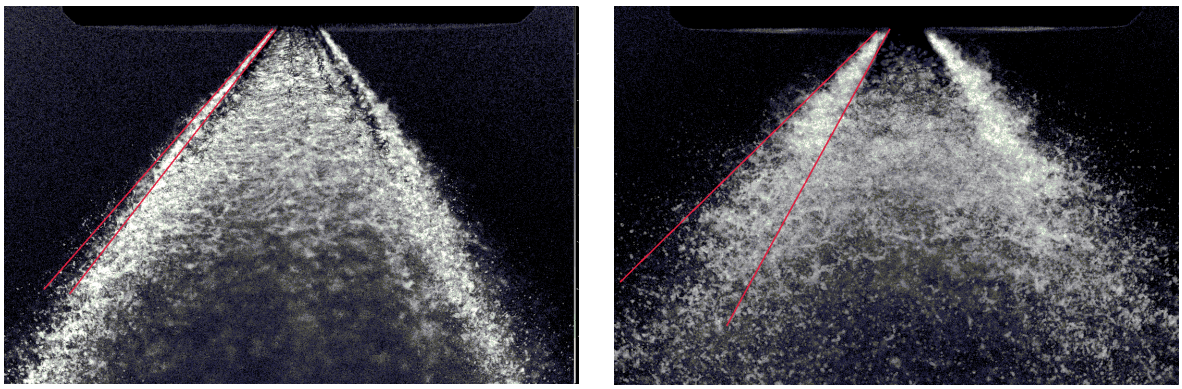

***Figure 6-7*** *Detection of the spray fluctuations using RMS images. Left is the stable atomizer, right is the unstable. Created from 10 images using shadowgraph.*

## 6.3 Influence of the atomizer design on the spray characteristics

Eleven atomizers were chosen to detailed PDA measurement. All measurements were done at inlet pressure 0.5, 1 and 1.5 MPa using kerosene Jet-A1 and two perpendicular axes in one axial distance from the atomizer with 35,000 samples or 30 s elapsed. Atomizers with spill-line were also tested at 1 MPa with spill to feed ratio of 0.4 and 0.8. Data, presented here, will be also published in [26].

### 6.3.1 Influence of the swirl chamber geometry

Five different swirl chamber were tested in the simplex atomizer. Four chamber have the same diameter of the exit orifice and they vary in the geometry of swirl chamber itself while the rest one have larger exit orifice. Several works have indicated that the internal flow in the swirl chamber is rather complex and proved the influence of the convergent exit shape on the inner flow [27, 28] but no one elucidate its impact on the resulting spray.

The spray images (Figure 6-8) show very little differences in the spray structure among various chamber shapes. The spray is stable for all the chambers. SCA seems to be independent on the chamber shape. The liquid sheet breakup starts at approximately equal distance except the chamber D where the breakup occurs rather closer to the exit orifice.

Radial profile of the velocities in Figure 6-9 well corresponds to the other observation of the hollow-cone sprays for each swirl chamber; the local maximum is expected in positions where the annular liquid sheet disintegrated. Tangential velocity is about one order of magnitude smaller for every tested atomizer and it descants further from the spray centre. The A and D chambers have slightly higher axial and radial velocities in position where the liquid sheet was presented. The AL chamber has shifted local maximum further from the spray centre. This corresponds to the same way shifted volume flow rate (Figure 6-10) and calculated cone angle in Table 6-1 which is noticeably wider than others. It corresponds to eq. (10) where the SCA is highly depended on the diameter of the exit orifice. Among other swirl chambers are nearly indistinguishable differences in SMD and SCA as well as in the flow characteristics. The variations of $C_D$ were typically less than 2%, with lowest $C_D$ found for the chamber C. The $C_D$ systematically (for all the chambers) varies with the inlet pressure as $C_D \propto \Delta p^{-0.035}$ as it was observed in the chapter 6.1. The variation of ISMD amongst the different chamber shapes was found to be surprisingly small, between ± 3%. Very similar trends were found for all the chambers, where ISMD $\propto \Delta p^{-0.255}$ – see Figure 6-11. The effect of the pressure on SCA is very small and not consistent amongst the chambers. In the case of the A and B chamber is evident rather decreasing slope while the D chamber shows insignificant increase in SCA. The C chamber behaves slightly different with strong ISMD decrease in the range of 0.5 and 1 MPa. Together with the noticeably increase in SCA in this particular pressure range it can be assumed that the internal flow is fully developed at higher pressure compared to the others swirl chambers. The velocity profiles from Figure 6-9 where the C chamber has relatively low axial velocity and the peak of the radial velocity is shifted further from the spray centre implies that that more pressure energy is transferred into radial velocity which results into wider spray cone.

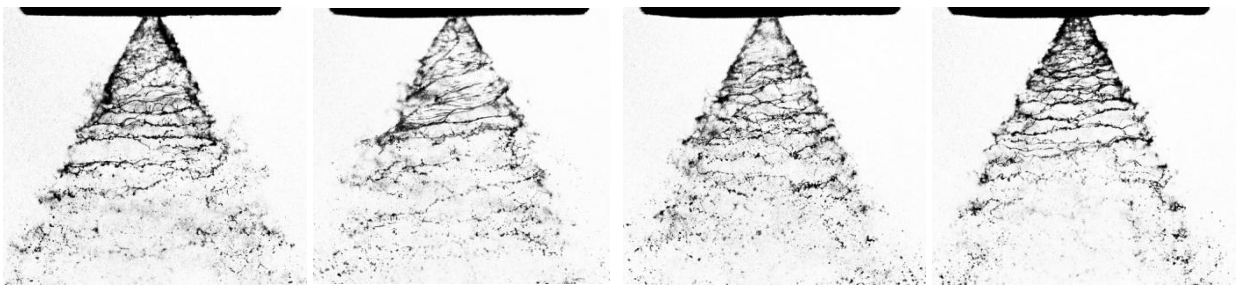

***Figure 6-8*** *Spray structure from various shaped swirl chambers. From left: A-SS, B-SS, C-SS and D-SS. 1 MPa*

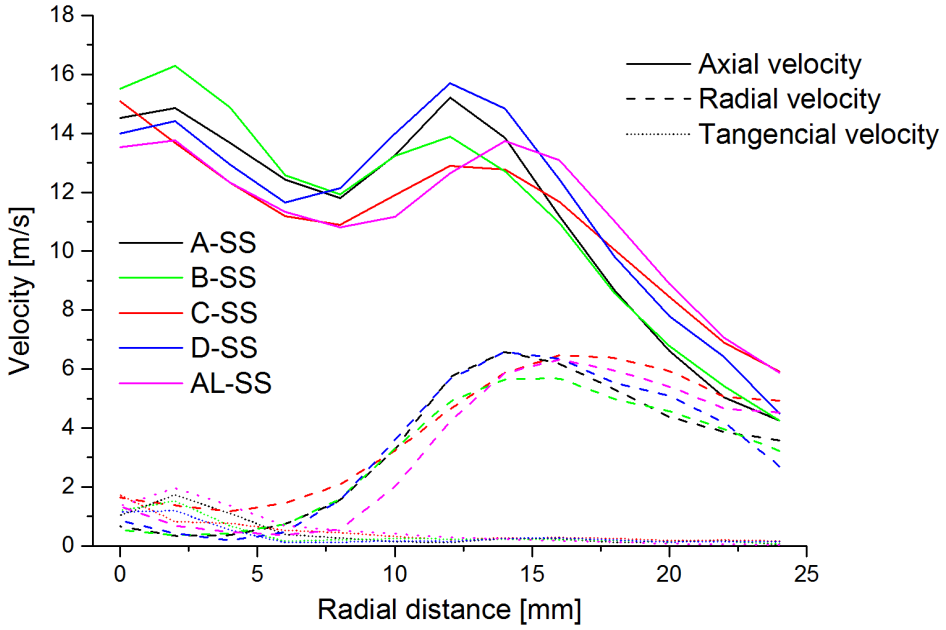


***Figure 6-9*** *Swirl chambers – velocities, 1 MPa*

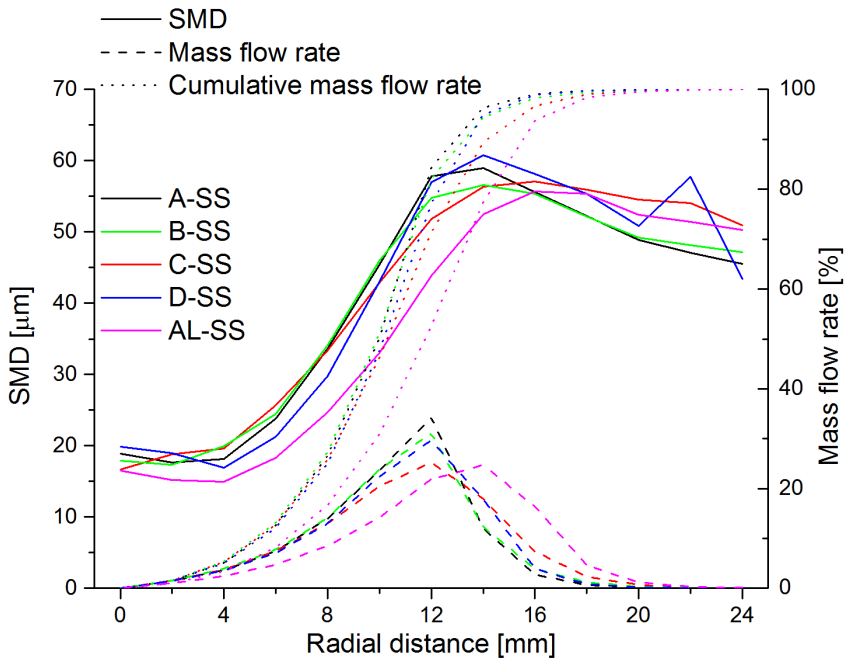


***Figure 6-10*** *Swirl chambers – SMD and mass flow rates, 1 MPa*

***Table 6-1*** *Swirl chambers - global characteristics for 1 MPa*

| Type | Mass flow rate | 1-50Hz, Median | $C_D$ | ISMD | Cone angle |
|---|---|---|---|---|---|
| [-] | [kg/h] | [Pa/MPa] | [-] | [µm] | [deg] |
| **A-SS** | 8.9 | 0.93 | 0.45 | 51.7 | 54.8 |
| **B-SS** | 8.7 | 0.40 | 0.44 | 49.7 | 56.0 |
| **C-SS** | 8.5 | 0.41 | 0.43 | 48.9 | 59.1 |
| **D-SS** | 8.8 | 0.24 | 0.44 | 51.9 | 56.5 |
| **AL-SS** | 10.3 | 0.80 | 0.44 | 47.8 | 63.7 |

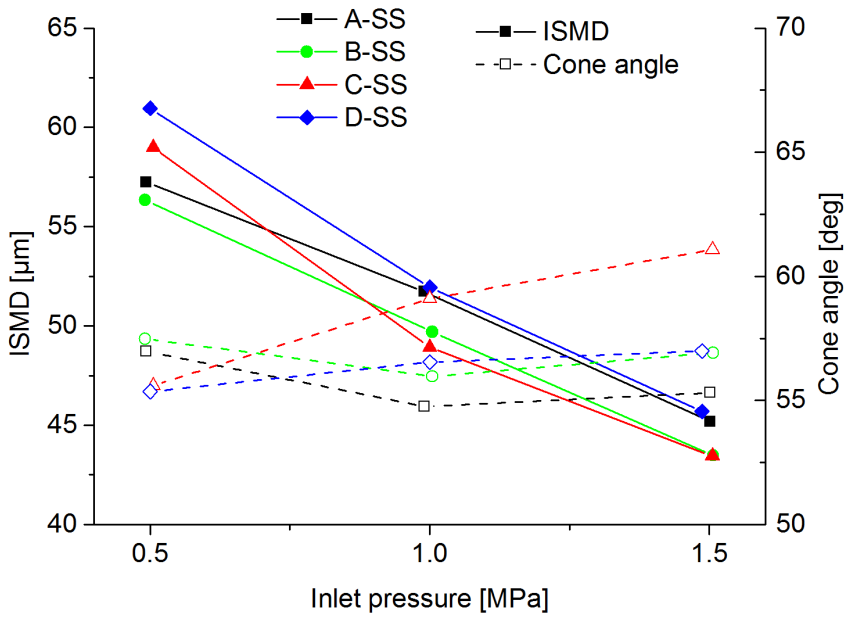


***Figure 6-11*** *Spray global characteristics - swirl chambers*

### 6.3.2 Influence of the tangential ports number

Three tangential entrees were tested varying only in the number of the ports. From data (Table 6-2) is evident decreasing mass flow rate with increasing number of ports due to greater pressure losses in smaller ports (the flow cross-section remains the same). The same trends were obtained for 0.5 and 1.5 MPa. The equivalent results were presented by Khavkin in [29].

Axial and radial velocity (Figure 6-12) is lower for atomizer with four ports due to the lowest mass flow rate among others. The SMD varies less than ± 2 % and variation in the liquid volume flux distribution (Figure 6-13) is almost imperceptible. However, calculated SCA is slightly increasing with greater number of the inlet ports.

Illustrative results of the circumferential patternation of the sprayed liquid are shown in Figure 6-14. The amount of liquid sprayed into the segments varies significantly, the flow rate differences among individual segments reach up to 50% of the mean value. These results show that the spray is considerably heterogeneous. The variation amongst all the segments can be described by the coefficient of variation. The coefficient of variation systematically decreases with the number of swirling inlets as well as with the inlet pressure, see Table 6-3. These findings are in accordance with [21, 29].

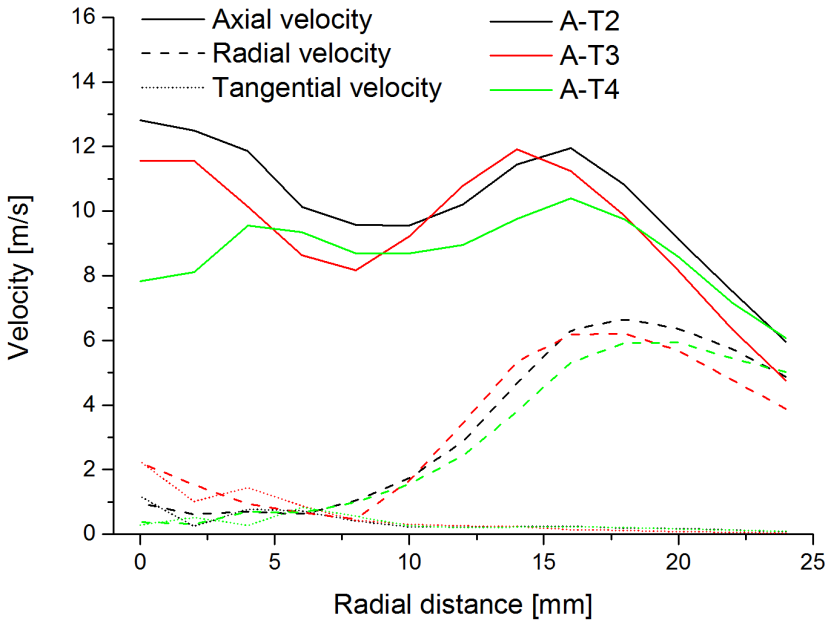


***Figure 6-12*** *Tangential ports – velocities, 1 MPa*

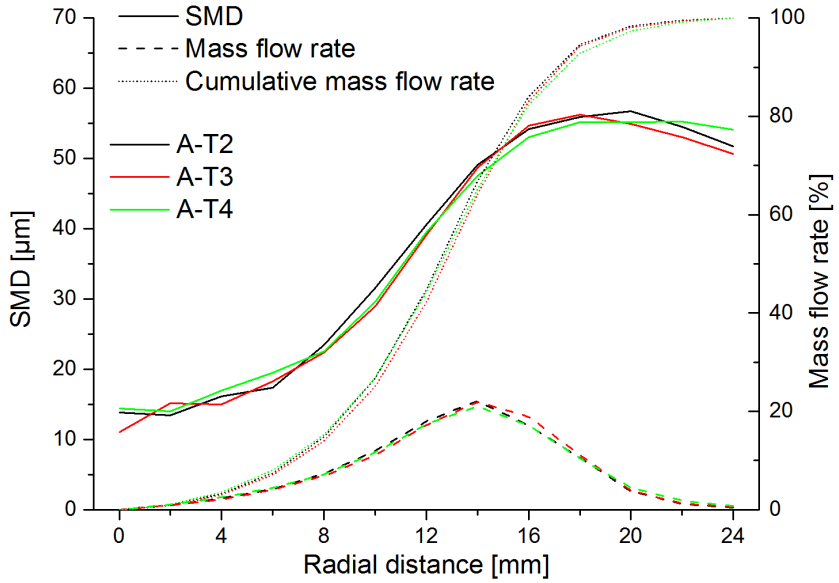


***Figure 6-13*** *Tangential ports - SMD and spray liquid distributions, 1 MPa*

***Table 6-2*** *Tangential ports - global characteristics, 1 MPa*

| Type | Mass flow rate | 1-50Hz, Median, | $C_D$ | ISMD | Cone angle |
|---|---|---|---|---|---|
| [-] | [kg/h] | [Pa/MPa] | [-] | [µm] | [deg] |
| **A-T2** | 8.3 | 0.92 | 0.36 | 48.0 | 67.0 |
| **A-T3** | 8.1 | 0.46 | 0.35 | 47.9 | 67.3 |
| **A-T4** | 7.0 | 0.62 | 0.31 | 47.1 | 69.3 |

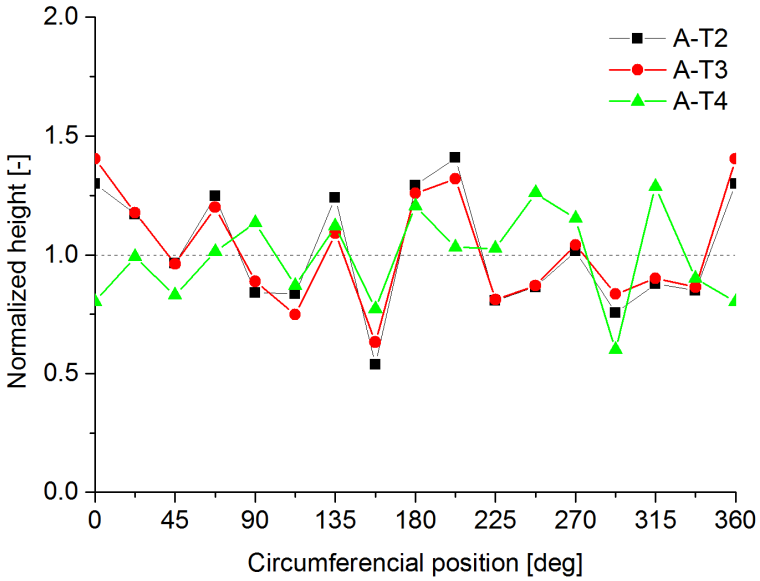


***Figure 6-14*** *Tangential ports - circumferential distribution*

***Table 6-3*** *Tangential ports - circumferential distribution*

| **Type** | **Inlet pressure** | | |
|---|---|---|---|
| **[-]** | **0.5 [MPa]** | **1 [MPa]** | **1.5 [MPa]** |
| **A-T2** | 0.31 | 0.24 | |
| **A-T3** | 0.29 | 0.22 | 0.18 |
| **A-T4** | 0.25 | 0.19 | |

### 6.3.3 Influence of the spill-line orifice geometry

The spill-return atomizers were rarely studied [30-35] and the effect of the spill-line orifice arrangement on the spray is not clear at all. Several different geometries (see chapter 5) of the spill-line orifices were tested in order to find its influence on the spray characteristics. Tests were done at 0.5, 1 and 1.5 MPa with closed spill-line which simulates atomizer's maximum power with great demands on the resulting spray and at 1 MPa with spill-feed ratio of 0.4 and 0.8.

Spray images show very similar behaviour of the off-axis SL orifices with closed SL. The axially placed SL orifice in S1 exhibits unstably. The low-profile S1LP performs better, however, the liquid sheet breaks more prior compared to the off-axis SL. In the spill regimes have both axially placed SL orifice very similar spray structure. Even small fractions (SFR 0.1) of the liquid spilled out lead to a steady spray from every tested atomizer. High SFRs show noticeable difference in the spray structure among tested SLs. The atomizers with the off-axis SL orifices have denser spray due to higher liquid injection rate – see Figure 6-16. In this work, the atomizer operation regime was driven by the spill-feed ratio as it is in real combustor. Due to this the liquid injection rate is different for each atomizer. The SL S4 has considerably the highest injection rates at both spill regimes but when the SL is closed, the mass flow rate is equivalent to others – see Table 6-4. The rest of the off-axis SLs have slightly lower flow rate but still about two times higher than the co-axis SLs in case of SFR

0.8. Therefore, it is necessary to change the operating point when the atomizer with the off-axis SL will be used.

The spray characteristics of the off-axis SLs (SFR 0) and the simplex atomizer are very similar to each other in terms of the velocities (Figure 6-17), SMD, liquid volume flux (Figure 6-18), ISMD and SCA (Figure 6-19). The differences are up to 1 % except small difference at 0.5 MPa where the simplex atomizer provides lower ISMD and wider spray cone. The presence of the off-axis SL orifice causes some additional energy loses inside the swirl chamber which are the most significant at the low pressure. Thus the simplex atomizer has higher velocities at this particular regime which causes wider SCA and consequently lower ISMD. The atomizers with the co-axis SL have greater diversions in the spray characteristics as well as in the spray stability. Atomizer with the SL S1 was found as unstable in every regimes and it had about 15 % higher $C_D$ than others – see Table 6-4. The S1LP was unstable up to approx. 0.9 MPa. Above 0.9 MPa is the stability improved which is evident on much lower $C_D$ and pressure fluctuations. The axial velocity of S1 is low but almost constant through the spray with faint local maximum. The SMD profile shows rather higher values around the spray centre, however, its lower further from the spray centre. The liquid volume distribution indicates wider spray cone which was confirmed by calculations. The ISMD is only slightly higher than the off-axis and simplex types at 0.5 MPa and the S1 has surprisingly the lowest ISMD at 1 MPa among all tested SLs.

The greater differences are found in regimes with spilled liquid, as it was outlined previously. When the SFR is increased, ISMD is decreasing and the SCA widens as it is shown in Figure 6-22. The only misbehaviour was found in case of S1 where SCA firstly decrease due to spray stabilizing. The S3 and S4 have noticeably higher ISMD and narrower spray in the regime of SFR 0.8 which will be discussed in detail. The S4 has the highest velocities with the local maximum closest to the spray center (Figure 6-20) as well as the highest SMD across whole spray (Figure 6-21). The S2 and S3 have similar velocities profiles to each other as well as the SCA and liquid volume distribution. The S1 and S1LP have the lowest velocities which are caused by the smallest liquid mass flow rate – see Table 6-5. The spray is characterized by the very wide cone and low SMD.

The application of the spill orifice placed out of the axis of the swirl chamber leads to the stable spray but it is redeemed by the necessity to change the operating conditions of the atomizers. Alternative solution is to use the obstacle in the spill line which is described in appendix B.

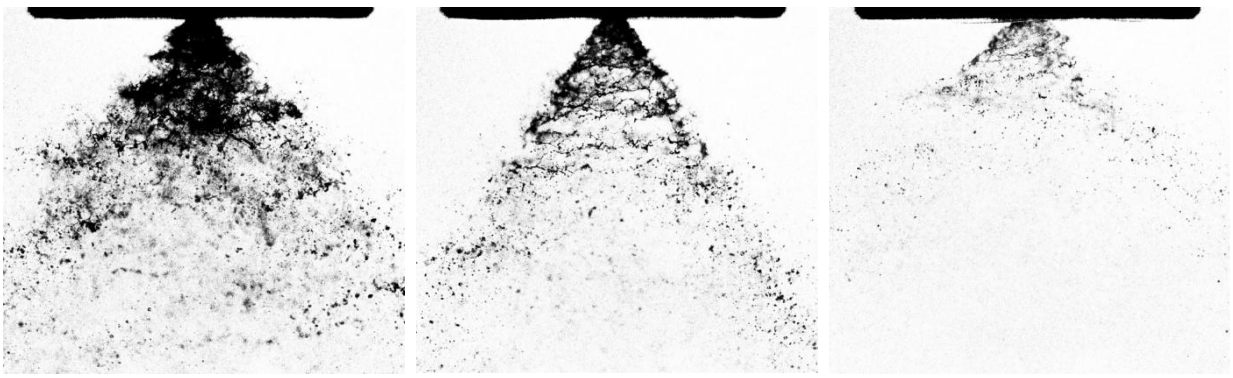

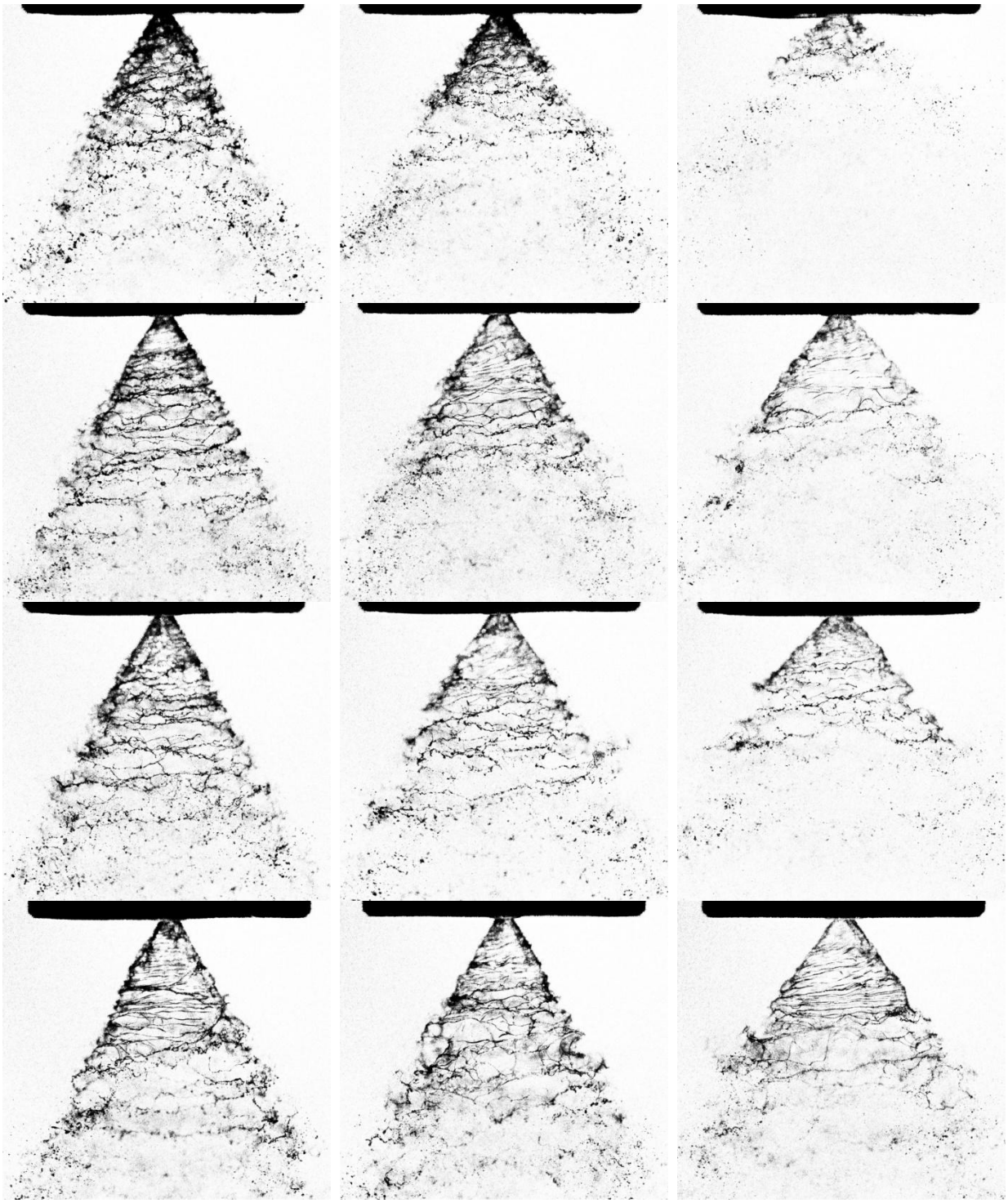

***Figure 6-15*** *Spray structure. From top: A-S1, A-S1LP, A-S2, A-S3 and A-S4. From left: 1 MPa SFR0, 1 MPa SFR 0,4 and 1 MPa SFR 0.8*

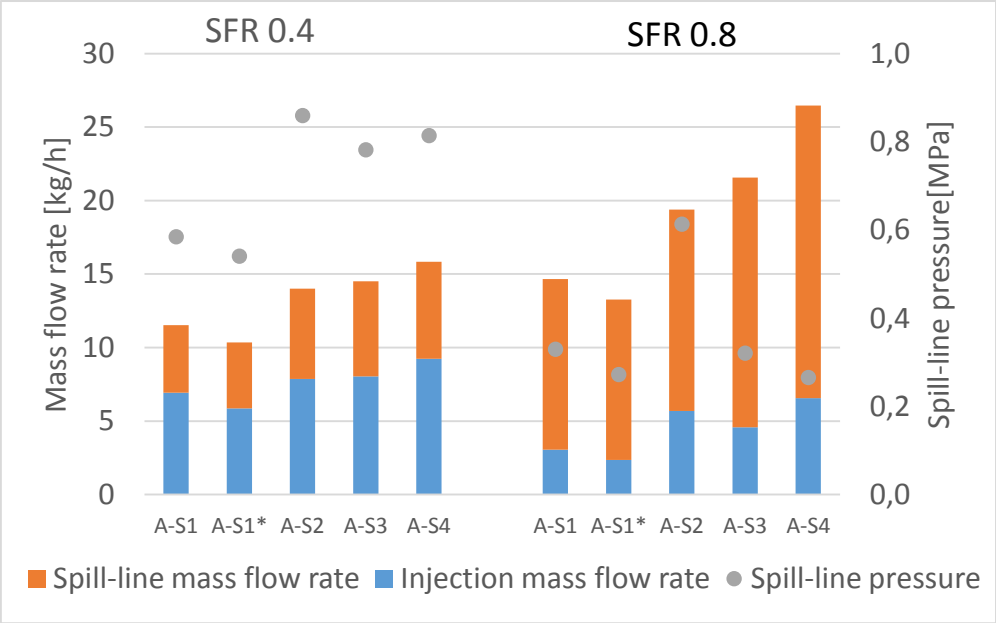


***Figure 6-16*** *Flow rates in the spill regimes at 1 MPa*

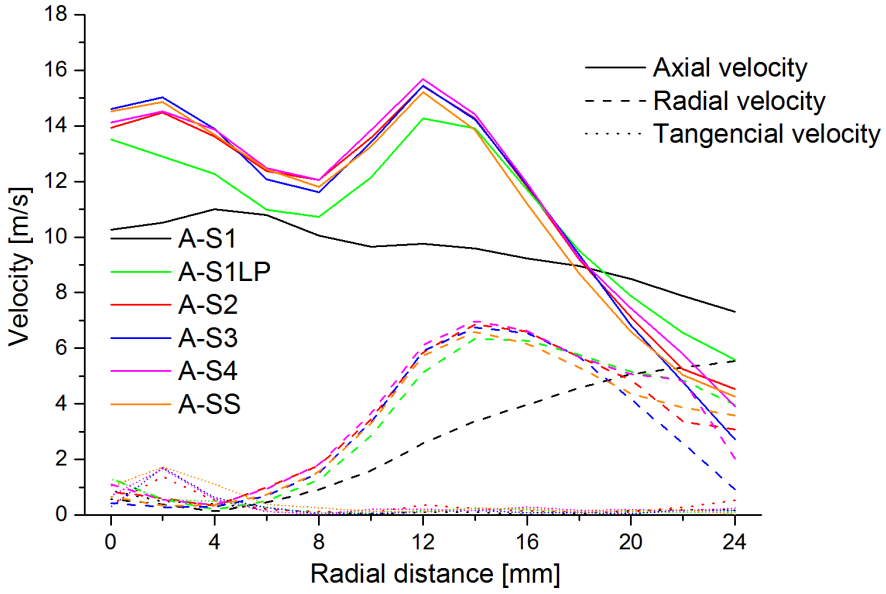


***Figure 6-17*** *Spill-line orifices – velocities, 1 MPa, SFR0*

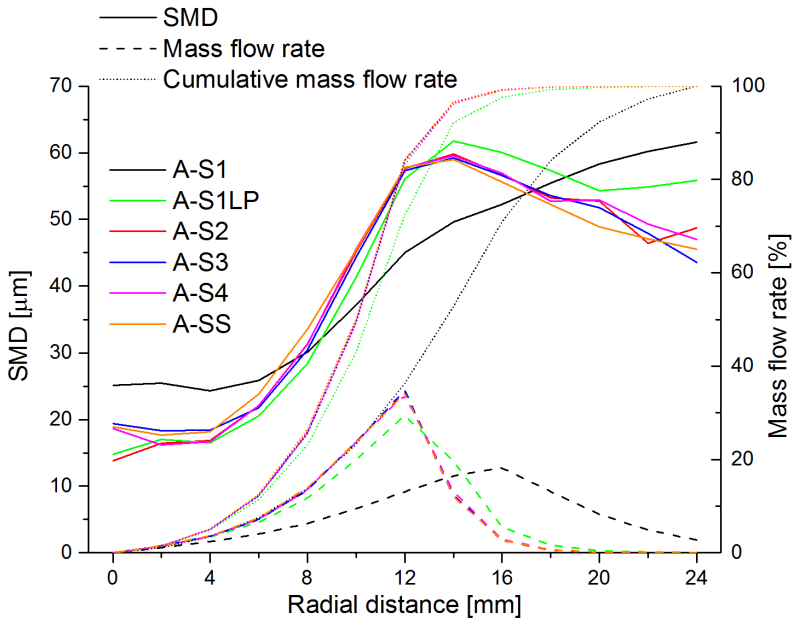


***Figure 6-18*** *Spill-line orifices - SMD and spray liquid distributions, 1 MPa, SFR0*

***Table 6-4*** *Spill-line orifices - global characteristics, 1 MPa, SFR0*

| Type | Spill-line pressure | Mass flow rate | 1-50Hz, Median, | $C_D$ | ISMD | Cone angle |
|---|---|---|---|---|---|---|
| [-] | [MPa] | [kg/h] | [Pa/MPa] | [-] | [µm] | [deg] |
| **A-S1** | 0.69 | 11.3 | 1.70 | 0.57 | 51.0 | 71.8 |
| **A-S1LP** | 0.72 | 9.0 | 1.49 | 0.45 | 52.4 | 57.7 |
| **A-S2** | 0.97 | 8.9 | 0.99 | 0.45 | 51.8 | 54.7 |
| **A-S3** | 0.97 | 9.2 | 0.48 | 0.46 | 51.4 | 54.8 |
| **A-S4** | 0.98 | 9.2 | 0.26 | 0.46 | 52.0 | 55.1 |
| **A-SS** | - | 8.9 | 0.93 | 0.45 | 51.7 | 54.8 |

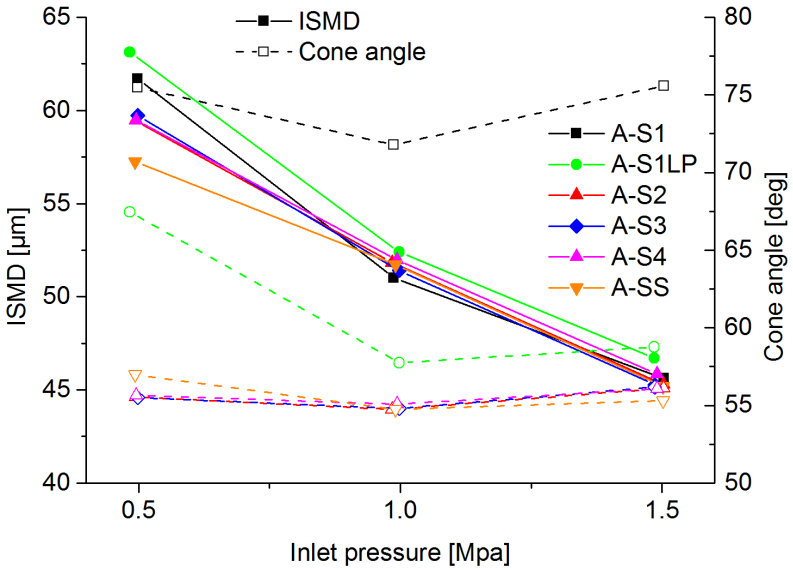


***Figure 6-19*** *Spray global characteristic - Spill-line orifices, pressure depended, SFR0*

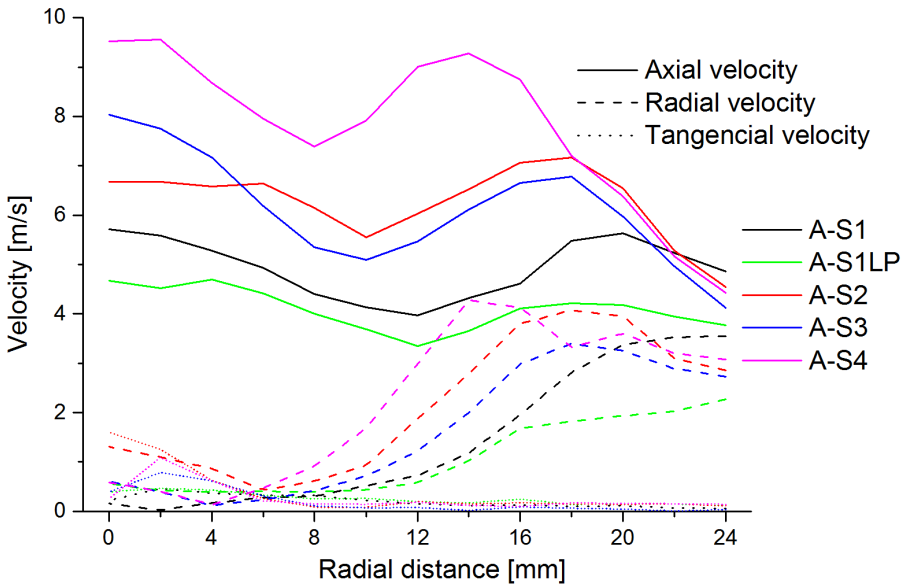


***Figure 6-20*** *Spill-line orifices – velocities, 1 MPa, SFR0.8*

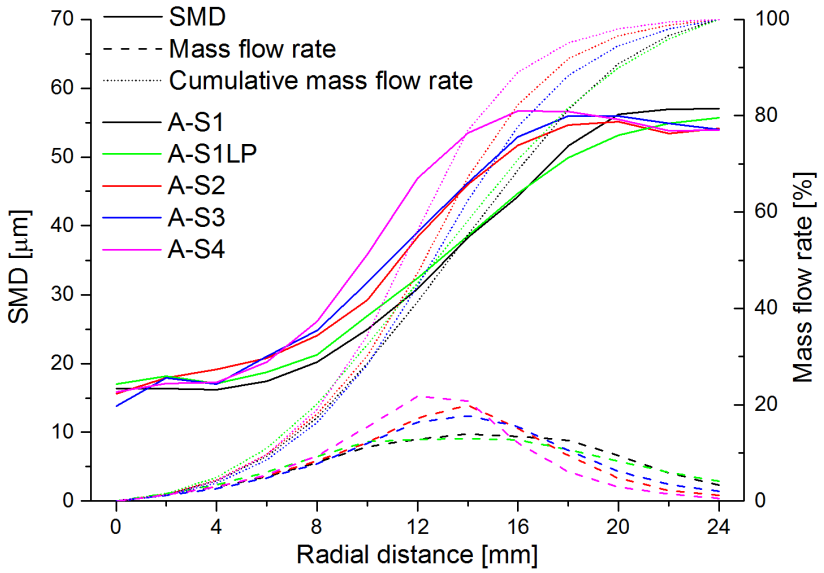


***Figure 6-21*** *Spill-line orifices – SMD and spray liquid distributions, 1 MPa, SFR0.8*

***Table 6-5*** *SL orifices - global characteristics, 1 MPa, SFR 0.8*

| Type | Spill-line pressure | Mass flow rate | Injection mass flow rate | 1-50Hz, Median | $C_D$ | ISMD | Cone angle |
|---|---|---|---|---|---|---|---|
| **[-]** | **[MPa]** | **[kg/h]** | **[kg/h]** | **[Pa/MPa]** | **[-]** | **[µm]** | **[deg]** |
| **A-S1** | 0.33 | 14.7 | 3.1 | 0.41 | 0.15 | 43.8 | 76.8 |
| **A-S1LP** | 0.27 | 13.3 | 2.4 | 1.43 | 0.12 | 42.5 | 77.4 |
| **A-S2** | 0.61 | 19.4 | 5.7 | 0.38 | 0.28 | 45.1 | 70.3 |
| **A-S3** | 0.32 | 21.6 | 4.6 | 0.65 | 0.23 | 46.8 | 73.1 |
| **A-S4** | 0.27 | 26.5 | 6.6 | 0.53 | 0.33 | 48.6 | 66.2 |

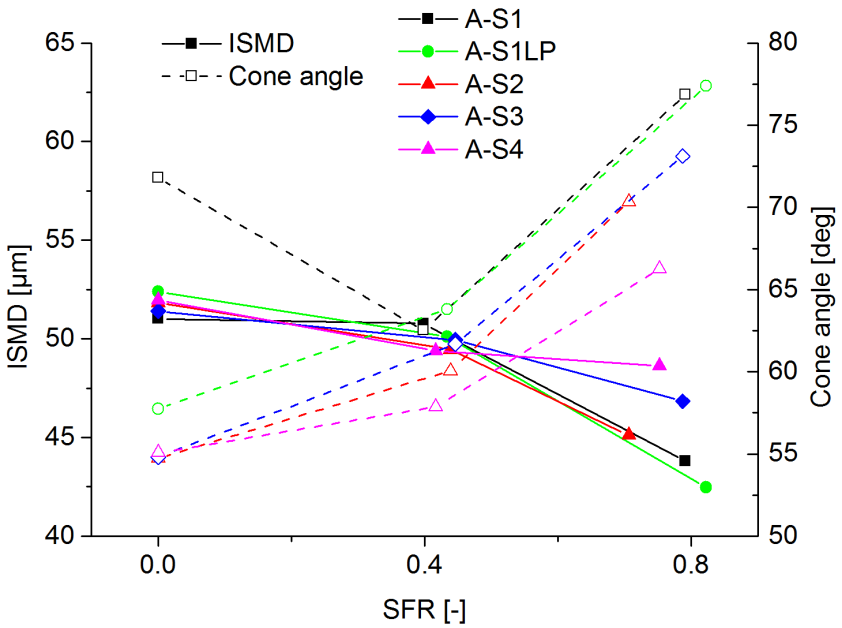


***Figure 6-22*** *Spray global characteristics - SL orifices - SFR dependent*

## 6.4 Correlation of ISMD on Reynolds number

The internal flow has strong influence on the resulting spray as it was investigated in previous text. Due to impossibility of direct velocity measurement inside the swirl chamber, the internal flow is considered as inviscid. The Reynolds number used here is the pressure based Reynolds number $Re_p$, where the velocity is expressed with the atomizing pressure and liquid density as:

$$V = \sqrt{\frac{2\Delta p}{\rho_l}} \tag{14}$$

which results in:

$$\mathrm{Re} = \frac{\sqrt{2\Delta p \rho_l}\, d_o}{\mu_l} \tag{15}$$

$Re_p$ was calculated for several pressure regimes and for various petroleum-based fuels from conference paper in appendix C. The ISMD decrease with $Re_p$ as ISMD $\propto Re_p^{-0.15}$ - see Figure 6-23. It is widely known that the drops become smaller with increasing liquid inertia and larger with increasing liquid viscosity. However, the liquid surface tension is not taken into calculations here and brings some level of uncertainty.

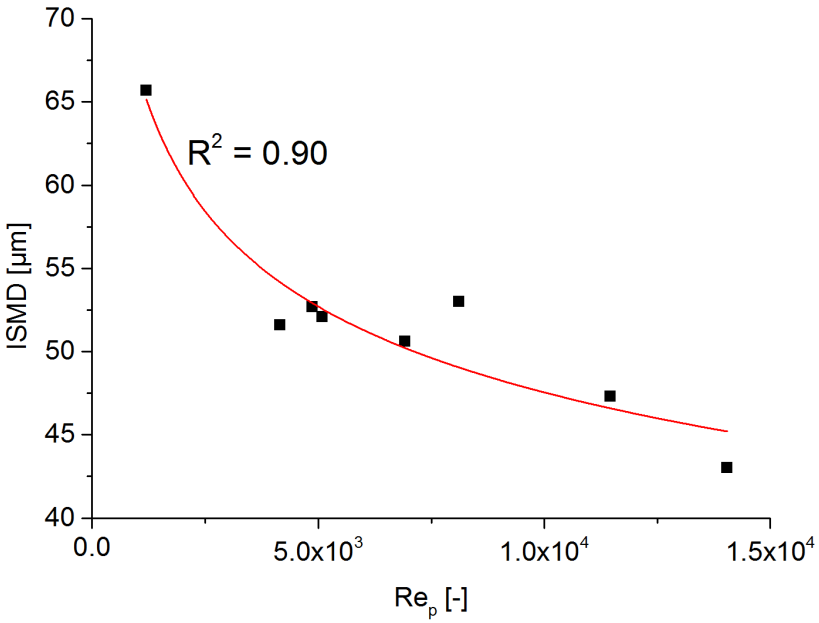


***Figure 6-23*** *Correlation of $Re_p$ and ISMD*

## 6.5 Quality of manufacture and fault conditions

It is impossible to manufacture an atomizer in unlimited precision; therefore, each part is produced with some tolerance and surface quality. Due to inability of the surface quality evaluation, dimensional precision and various fault states will be only evaluated.

### 6.5.1 Dimensional evaluation

Dimensional tolerances have a significant influence on a price of fabrication [36] as well as on a spray mass flow rate (eq.7). Basic dimensions were measured using a microscopic image (see Figure 6-24) from an optical microscope Nikon Eclipse E200. Dimensions were established with estimated deviation of 0.001 mm and compared with a drawing documentation.

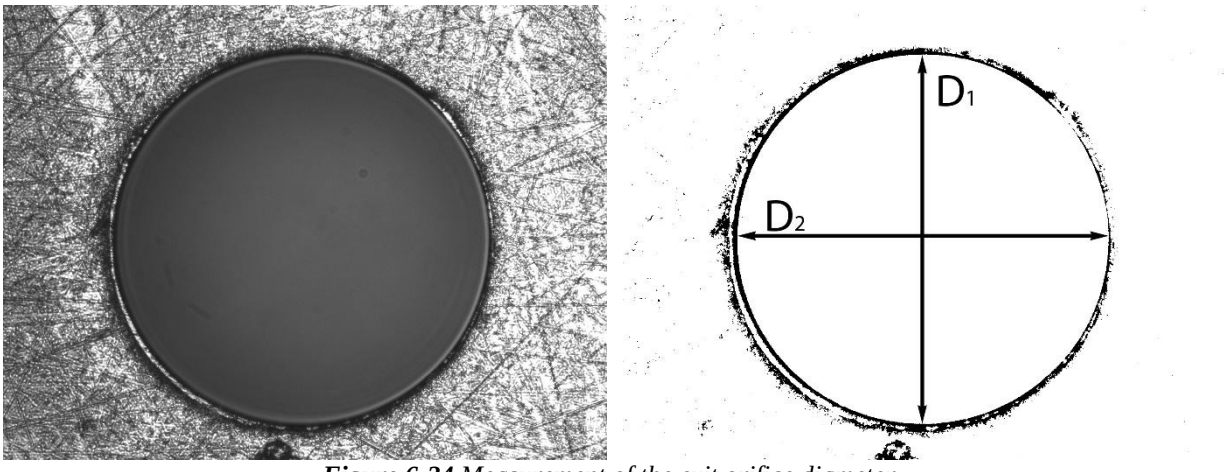


***Figure 6-24*** *Measurement of the exit orifice diameter*

Precision of manufacture may, inter alia, affect the liquid mass flow across the exit orifice. Combining equations 6 and 7 results in a semi-empirical correlation between the liquid low rate and atomizers dimensions:

$$\dot{m}_l = 0.35\left(\frac{A_p}{d_s d_o}\right)^{0.5}\left(\frac{d_s}{d_o}\right)^{0.25} A_0\sqrt{2\rho_l \Delta p} \tag{16}$$

Assuming the same operating conditions (same inlet pressure and liquid properties):

$$M = 3.64\frac{\dot{m}_l}{\sqrt{2\rho_l \Delta p}} = \frac{A_p^{0.5} d_o^{1.25}}{d_s^{0.25}} \tag{17}$$

where $M$ represents unit flow rate.

It is obvious that the exit orifice diameter has the largest contribution on the liquid flow rate, whereas the swirl chamber diameter has only minor influence.

The size measurements endorse that each measured component meets the accuracy requirements specified in the drawing; e.g.: the prescribed tolerance of the exit orifice diameter was $0.42^{+0}_{-0.01}$ and measured dimension were 0.419, 0.416 and 0.411. When the most extreme scenarios based on the tolerance bands ($d_s = 3^{+0.05}_{-0}$, $b_p = h_p = 0.6^{+0.05}_{-0}$) are taken into account, from eq. 17 it is possible to estimate changes in the flow rate. Mean theoretical flow rate (for the atomizer A-SS) is $M = 2.23 \cdot 10^{-7}$, the bottom extreme is $M = 2.11 \cdot 10^{-7}$, the top extreme is $M = 2.36 \cdot 10^{-7}$ which corresponds to the flow of the kerosene at 1 MPa of 8.80, 8.31 and 9.35 kg/h respective. The difference between both extremes is 12.1 %. If the more atomizers operate together, their match is recommended.

### 6.5.2 Surface damage

One of the investigated atomizers has mechanically disrupted surface of the inlet ports (Figure 6-25). The spray from the corrupted atomizer is considerably more heterogeneous with coefficient of variations $c_v$ of the liquid distribution ($c_v = 0.43$) almost twice as strong than an atomizer of the same geometry with good quality surface ($c_v = 0.24$). For circumferential profile see Figure 6-26.

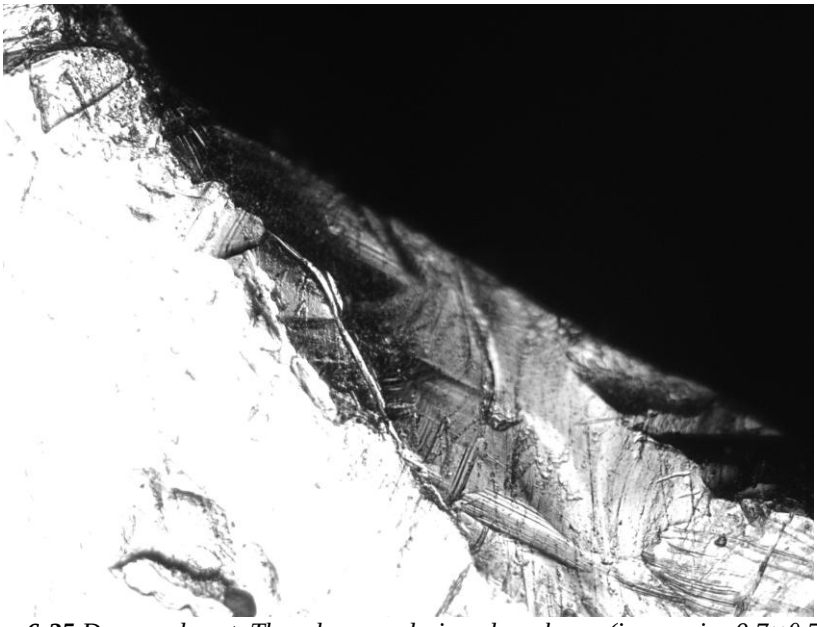

***Figure 6-25*** *Damaged port. The edge was designed as sharp. (image size 0.7×0.7 mm)*

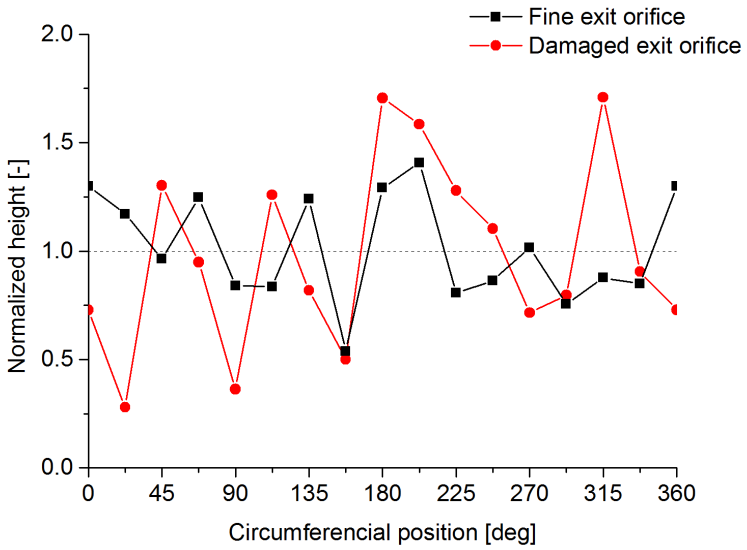


***Figure 6-26*** *Circumferential distribution - fine and damaged exit orifice*

### 6.5.3 Fault conditions

The fault condition may occur when the atomizers inner parts are blocked, deformed or displaced. The consequences of the blocked exit orifice are obvious – liquid flow rate is disturbed and the atomizer fails in its task. The behaviour of the blocked SL orifice is less known, mostly due to unimportance of dealing with this problem due to much larger diameter of the SL orifice in compare to the exit orifice diameter. However, when the off-axis SL orifices are used, their diameter is very close to the diameter of the exit orifice or it is even smaller thus the danger of blocking must be taken into account. If one of the off-axis SL orifices is blocked out, spilled liquid flows only through the free orifice and the spray becomes very unsymmetrical – see Figure 6-27.

Another fault condition was observed in the case of simplex atomizers when the pressure difference between the inlet and the spill-line exceeded 1 MPa. The pressure force acting on the cap was larger than the force of bias spring that keep the cap in the position. Therefore, the inlet flow cross-section as well as the liquid flow rate increases rapidly as it is shown in Figure 6-28. The atomizer's body is primary designed to operate with the spill-line and this behaviour cannot occur in standard condition. Nevertheless, the body must be redesigned if there will be an interest to operate these atomizers as simplex.

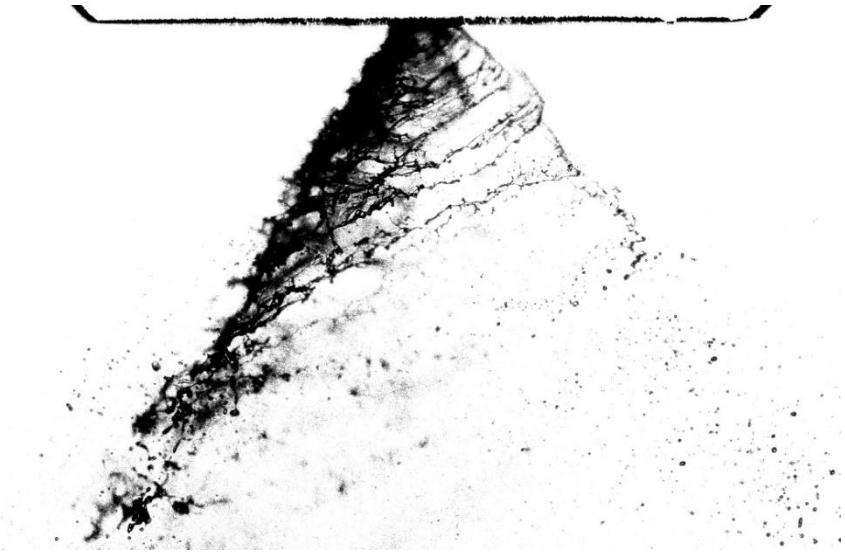

***Figure 6-27*** *Fault state of off-axis spill-line atomizer, 10 bar SFR 0.8*

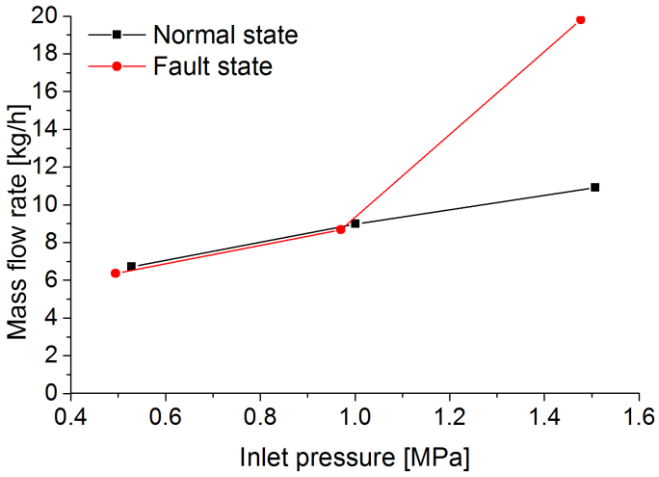


***Figure 6-28*** *Cap failure, simplex atomizer*

# 7 Conclusion

The present work investigated the effects of the atomizer geometry on the final spray structure and stability. The effect of entry ports number, swirl chamber shape and spill-line orifice design were investigated together with evaluation of the manufacturing precision.

The tests were made with Jet A-1 fuel as the test liquid at inlet pressures of 0.5, 1.0 and 1.5 MPa, and additionally, for the atomizers with spill return orifice, also at inlet over-pressure of 1.0 MPa for SFRs of 0.4 and 0.8. The atomizer characteristics were analysed and discussed by means of spray characteristics such as a droplet size in the spray, velocity distributions and the spray cone angle, or by atomizer characteristics such as pressure pulsation levels and discharge coefficients.

Only small differences were found amongst the simplex atomizers with different swirl chamber shape in terms of flow rate, cone angle, droplet size and velocity.

Atomizers with two, three and four tangential entry ports have been compared and found very similar in terms of droplet size and velocity. The circumferential liquid distribution has shown that the spray is markedly heterogeneous. The spray uniformity systematically improves with the number of swirling inlets as well as with the inlet pressure.

The spill-line geometry plays an important role in spray stability. The atomizers with axial spill orifice perform strong spray pulsations in regimes with the SR closed while the atomizers with the off-axis spill orifices produce a stable spray. Periodical decays of the air core have been suggested as the pulsation reason. Atomizer with unstable spray has the $C_D$ notably higher than the stable atomizer. This behaviour was, together with subjective observations and pressure pulsations in the inlet line, used to determine whether the spray is stable or not.

The optimized atomizer uses a three or four inlet ports with the off-axis spill orifices (S2).

# Bibliography

[1] Lefebvre, A. H., 1989, Atomization and sprays, Hemisphere Pub. Corp., New York.

[2] Zaremba, M., 2013, "Influence of operation conditions on spray characteristics of twin fluid atomizers," Masters Thesis, Brno University of Technology, Brno.

[3] Durdina, L., 2012, "Measurement of spray characteristics using optical measurement methods," Master thesis, Brno University of Technology, Brno.

[4] Malý, M., 2014, "Quality of fuel atomization from small pressure-swirl atomizers," Bachelor thesis, Brno university of technology, Brno.

[5] Ashgriz, N., and SpringerLink (Online service), 2011, "Handbook of atomization and sprays: Theory and applications," Springer,, New York, pp. xvi, 935 p.

[6] Sirignano, W. A., and Mehring, C., 2000, "Review of theory of distortion and disintegration of liquid streams," Progress in Energy and Combustion Science, 26(4–6), pp. 609-655.

[7] Strutt, J. W., and Rayleigh, L., 1878, "On the instability of jets," Proc. London Math. Soc, 10, pp. 4-13.

[8] Lin, S. P., 2003, Breakup of Liquid Sheets and Jets, Cambridge University Press.

[9] Guildenbecher, D. R., López-Rivera, C., and Sojka, P. E., 2009, "Secondary atomization," Experiments in Fluids, 46(3), pp. 371-402.

[10] Schmehl, R., "Modeling droplet breakup in complex two-phase flows," Proc. ICLASS Conference, Sorento, Italy.

[11] Qian, J., and LAW, C. K., 1997, "Regimes of coalescence and separation in droplet collision," Journal of Fluid Mechanics, 331, pp. 59-80.

[12] Crowe, C. T., 2005, Multiphase flow handbook, CRC press.

[13] Lefebvre, A. H., and Ballal, D. R., 2010, "Gas turbine combustion," Taylor & Francis,, Boca Raton, pp. 1 online resource (xix, 537 p.).

[14] Rizk, N. K., and Lefebvre, A. H., 1985, "Internal flow characteristics of simplex swirl atomizers," Journal of Propulsion and Power, 1(3), pp. 193-199.

[15] Jedelsky, J., and Jicha, M., 2014, "Energy considerations in spraying process of a spill-return pressure-swirl atomizer," Applied Energy, 132, pp. 485-495.

[16] Ballester, J., and Dopazo, C., 1994, "Discharge coefficient and spray angle measurements for small pressure-swirl nozzles," Atomization and sprays, 4(3).

[17] Albrecht, H.-E., 2003, Laser doppler and phase doppler measurement techniques, Springer, Berlin ; New York.

[18] Zhang, Z., 2010, LDA Application Methods: Laser Doppler Anemometry for Fluid Dynamics, Springer.

[19] Lading, L., Wigley, G., and Buchhave, P., 1994, Optical diagnostics for flow processes, Plenum Press.

[20] "Dantec Dynamics. [online]," http://www.dantecdynamics.com.

[21] Chen, S., Lefebvre, A., and Rollbuhler, J., 1993, "Factors influencing the circumferential liquid distribution from pressure-swirl atomizers," Journal of engineering for gas turbines and power, 115(3), pp. 447-452.

[22] Lan, Z., Zhu, D., Tian, W., Su, G., and Qiu, S., 2014, "Experimental study on spray characteristics of pressure-swirl nozzles in pressurizer," Annals of Nuclear Energy, 63, pp. 215-227.

[23] Rashid, M. S. F. M., Hamid, A. H. A., Sheng, O. C., and Ghaffar, Z. A., 2012, "Effect of Inlet Slot Number on the Spray Cone Angle and Discharge Coefficient of Swirl Atomizer," Procedia Engineering, 41, pp. 1781-1786.

[24] Silva Couto, H., Lacava, P. T., Bastos-Netto, D., and Pimenta, A. P., 2009, "Experimental Evaluation of a Low Pressure-Swirl Atomizer Applied Engineering Design Procedure," Journal of Propulsion and Power, 25(2), pp. 358-364.

[25] Datta, A., and Som, S., 2000, "Numerical prediction of air core diameter, coefficient of discharge and spray cone angle of a swirl spray pressure nozzle," International journal of heat and fluid flow, 21(4), pp. 412-419.

[26] Jedelsky, J., Malý, M., Janáčková, L., and Jícha, M., In press, "Effect of Geometric Factors on Spray Characteristics and Stability for Small Spill-Return Pressure-Swirl Atomizers," ILASS 2016Brighton, p. 12.

[27] Xue, J., Jog, M. A., Jeng, S. M., Steinthorsson, E., and Benjamin, M. A., 2004, "Effect of geometric parameters on simplex atomizer performance," Aiaa Journal, 42(12), pp. 2408-2415.

[28] Cooper, D., Yule, A., and Chinn, J., "Experimental measurements and computational predictions of the internal flow field in a pressure swirl atomizer," Proc. Proc. ILASS-Europe.

[29] Khavkin, Y., 2004, The Theory and Practice of Swirl Atomizers, Taylor & Francis.

[30] Carey, F. H., 1954, "The Development of the Spill Flow Burner and Its Control System for Gas Turbine Engines," Journal of the Royal Aeronautical Society, 58, pp. 737-753.

[31] Kapitaniak, A., 1967, "The Influence of Chosen Construction Parameters on the Performance of Spill-Control Pressure-Jet Atomizers," Journal of the Institute of Fuel, pp. 24-35.

[32] Loffler-Mang, M., and Leuckel, W., 1991, "Atomization with Spill-Controled Swirl Pressure-Jet Nozzles," ICLASS-91, Gaithersburg, MD, USA, pp. 431-440.

[33] Nasr, G., Yule, A., Stewart, J., Whitehead, A., and Hughes, T., 2011, "A new fine spray, low flowrate, spill-return swirl atomizer," Proceedings of the Institution of Mechanical Engineers, Part C: Journal of Mechanical Engineering Science, 225(4), pp. 897-908.

[34] Rizk, N., and Lefebvre, A., 1985, "Drop-size distribution characteristics of spill-return atomizers," Journal of Propulsion and Power, 1(1), pp. 16-22.

[35] Rizk, N., and Lefebvre, A., 1985, "Spray characteristics of spill-return atomizers," Journal of Propulsion and Power, 1(3), pp. 200-204.

[36] Chase, K. W., and Greenwood, W. H., 1988, "Design issues in mechanical tolerance analysis," Manufacturing Review, 1(1), pp. 50-59.

# List of symbols

Roman symbols

| | | |
|---|---|---|
| $A_p$ | Total area of inlet tangential ports | [$m^2$] |
| $A_o$ | Area of exit orifice | [$m^2$] |
| $B$ | Impact parameter | [-] |
| $b_p$ | Width of inlet tangential port | [m] |
| $C_D$ | Discharge coefficient | [-] |
| $D_{20}$ | Area mean diameter | [m] |
| $D_{30}$ | Volume mean diameter | [m] |
| $D_{32}$ | Sauter mean diameter | [m] |
| $d_c$ | Diameter of swirl chamber | [m] |
| $d_0$ | Diameter of exit orifice | [m] |
| $d_s$ | Diameter of SL orifice | [m] |
| E | Error of measuring device | [%] |
| $f_d$ | Doppler frequency | [Hz] |
| $f_i$ | Data rate | [Hz] |
| $h_p$ | Height of inlet tangential port | [m] |
| $h_c$ | Height of swirl chamber | [m] |
| $l_c$ | Length of swirl chamber | [m] |
| $l_o$ | Length of orifice | [m] |
| $l_p$ | Length of tangential port | [m] |
| We | Weber number | [-] |
| Re | Reynolds number | [-] |
| $Re_p$ | Pressure based Reynolds number | [-] |
| Oh | Ohnesorge number | [-] |
| $\dot{m}_l$ | Liquid mass flow rate | [kg/s] |
| $t$ | Time | [s] |
| $t^*$ | Characteristic deformation time | [s] |
| $S_s$ | Pitch of spill-line orifices | [m] |
| $U$ | Velocity of the particle normal to the fringes | [m/s] |

Greek symbols

| | | |
|---|---|---|
| $\Delta p_l$ | Injector pressure differential | [Pa] |
| $\sigma$ | Surface tension | [kg/s$^2$] |
| $\rho_l$ | Liquid density | [kg/m$^3$] |
| $\rho_g$ | Gas density | [kg/m$^3$] |
| $\theta$ | Spray cone angle | [deg] |
| $\theta_b$ | Angle between the laser beams | [deg] |
| $\mu_l$ | liquid dynamic viscosity | [Pa·s] |
| $\delta_f$ | Fringe spacing | [m] |
| $\chi$ | Separation distance between droplets centre | [m] |

Abbreviations

| | | |
|---|---|---|
| ISMD | Integral Sauter mean diameter | [m] |
| LDA | Laser Doppler anemometry | |
| PDA | Phase Doppler anemometry | |
| PS | Pressure-swirl | |
| RMS | Root mean square | |
| SL | Spill-line | |
| SMD | Sauter mean diameter | [m] |

# A. Conference paper at HydroTermo 2015

**Reference**:

MALÝ, M.; JANÁČKOVÁ, L.; JEDELSKÝ, J.; JÍCHA, M. Experimental investigation of pressure-swirl atomizers with a modification in a geometry of spill- return orifice. In *34th Conference of Departments of Fluids Mechanics and Thermomechanics Proceedings of Extended Abstracts.* 1. Litoměřice: 2015. s. 1-2. ISBN: 978-80-7414-912- 2.

**SKMTaT 2015, 23-25 June, 2015**
J. E. Purkyně University in Ústí nad Labem,
Faculty of Production Technology and Management,
Department of machines and mechanics,
Ústí nad Labem, Czech Republic

# Experimental investigation of pressure-swirl atomizers with a modification in a geometry of spill-return orifice

Milan Malý[1], Lada Janáčková, Jan Jedelský, Miroslav Jícha

***Keywords:*** Spill-return atomizer, Phase Doppler Anemometry, shadowgraphy

## 1. Introduction

A spill return atomizer is basically a pressure swirl atomizer, which contains a passage in the rear wall of the swirl chamber known as a spill-return orifice. Liquid is injected via tangential ports to the swirl chamber, where is divided into two streams, one is discharged to the outside and atomized, the second is "spilled" back to the reservoir. An amount of spilled fuel is regulated by a control valve in a spill-return line.

Fuel is always supplied to the swirl chamber at high pressure, providing good atomization over a wide span of injection flow rate. This nature is allowing to use the spill-return atomizers in applications requiring the wide regulation range such as industrial burners and gas turbine combustors [1].

Two small sized spill-return swirl atomizers were chosen for this study. Both of them have the same geometry varying only in the spill-return orifice geometry. The former atomizer uses the direct axial spill-return orifice located in a centre of the swirl chamber. Several modifications were made in order to reduce spray fluctuations and improve atomization quality. One solution, examined in this work, is represented by the modified atomizer containing an obstacle blocking direct axial flow through the spill-return orifice.

## 2. Experimental setup

Experiments were performed at a specially designed facility for spray generation under controlled conditions in the Spray laboratory at the Brno University of Technology.

Operation regime of the atomizer was controlled by setting the inlet pressure to 1 MPa. The spill line was closed by the valve near the atomizer. Droplet sizes and velocities were probed by two component fiber PDA Dantec dynamics. PDA measurement was made at axial distance Z=10 mm from the exit orifice. Two perpendicular axes with 15 positions were measured. In every position, 200,000 samples or 60 seconds were taken.

Spray images were taken by Canon EOS D300 with Canon EF 100 mm f/2.8 UMS Macro lens fitted on 68 mm long extension tube. The spray was illuminated by Nd:YAG NewWave Research Gemini laser with pulse duration of 5 ns and energy of pulse of 5 mJ. Imaging system was configured as shadowgraph, simplified scheme is shown in Fig. 1.

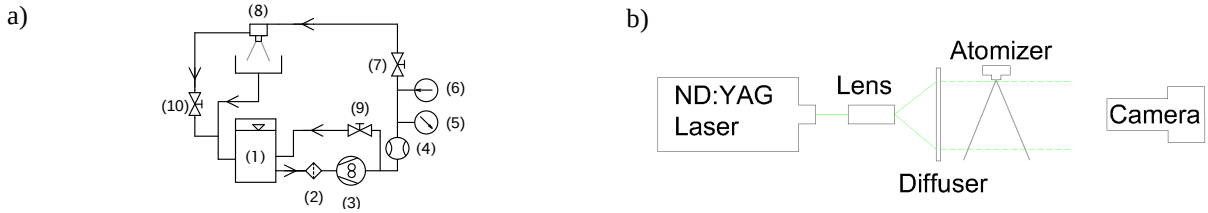


**Fig. 1** a) Schematic layout of fuel circuit, b) arrangement of shadowgraph

## 3. Results and discussion

The first estimation of spray characteristics was made by subjective observation, finding that the former atomizer is fluctuating at rate about 15 Hz and the modified is very stable. For better understanding of the break-up, detailed spray images were taken. There is an evident disparity between modified and former atomizer (Fig. 2). The stable geometry has well defined liquid sheet, disintegrating about 3 mm from the exit orifice, whereas the

[1] [1] Faculty of Mechanical Engineering, Brno University of Technology. Technická 2896/2, Brno 61669, Czech Republic. E-mail: milanmaly@email.com

unstable atomizer break-up practically randomly, depending on state of pulse, liquid sheet as well as chaotic mode of break-up may occur.

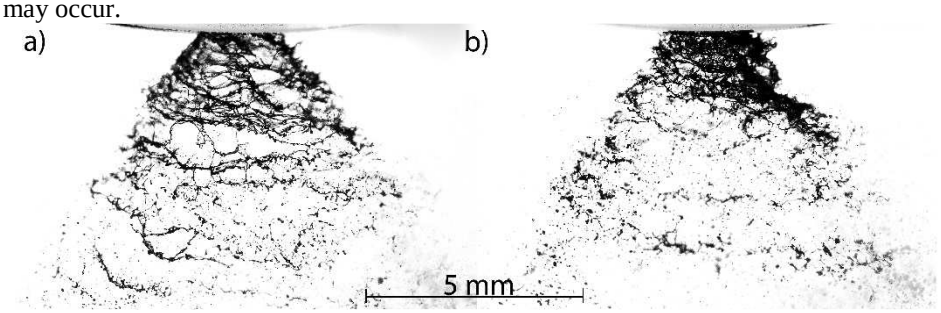


**Fig. 2** Shadowgraph images of a) Modified atomizer b) Former atomizer

PDA data in Fig. 3 shows significant difference in positions near the spray center, where the unstable atomizer has higher Sauter mean diameter and lower axial velocity. The particle velocity data from center of the spray were used for estimation of fluctuating frequency.

The behavior of the former atomizer is possibly caused by instabilities of the air core inside the swirl chamber according to finding of Kim et al in [2]. They found, that the long air core (the long swirl chamber) is acting more unstable compared to the shorter one. In our study, the same swirl chamber was used for both atomizers, but it could be assumed that the air core passed through the spill return orifice. In the modified atomizer, which is using an obstacle blocking direct axial flow, air core is terminated by the obstacle, thus the modified atomizer is more stable than the former with longer air core.

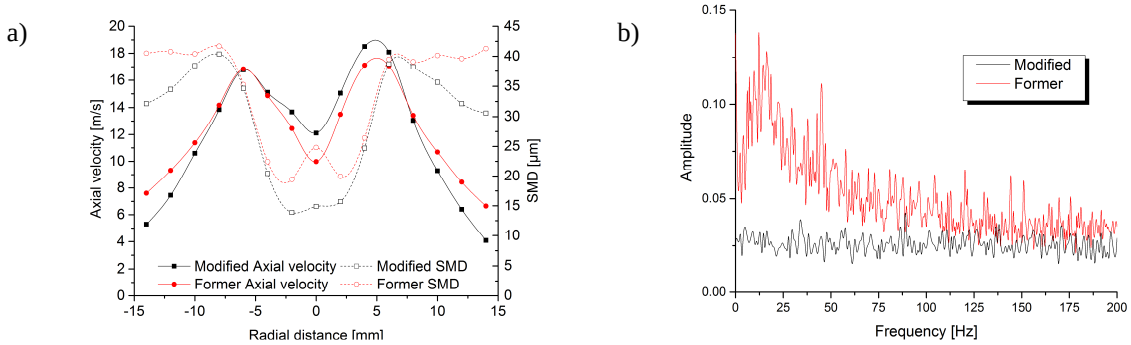


**Fig. 3** a) Spray profile characteristics b) FFT from PDA data

## 4. Conclusions

The new design of the spill-return orifice presented here is resulting in more stable and finer spray. The examination of experimental data together with spray images are pointing out some instabilities of the inner flow caused by fluctuating of the air core in case of the former atomizer.

A lot of works about an influence of the pressure-swirl atomizer geometry on spray were published, but just a few of them were inspecting an effect of the geometry of the spill-return orifice. This paper is a brief introduction to this phenomena indicating necessity of further investigation.

## Acknowledgement

This work has been supported by the project No. GA15-09040S funded by the Czech Science Foundation and the project LO1202 NETME CENTRE PLUS with the financial support from the Ministry of Education, Youth and Sports of the Czech Republic under the "National Sustainability Programme I".

## References

[1] Lefebvre, A. H.: *Atomization and sprays. Hemisphere Pub. Corp.*, New York.
[2] Kim, S., Khil, T., Kim, D., and Yoon, Y.:*Effect of geometric parameters on the liquid film thickness and air core formation in a swirl injector*. Measurement Science and Technology, 20(1), p. 015403.

# B. Conference paper at EFM 2015

**Reference:**

MALÝ, M.; JANÁČKOVÁ, L.; JEDELSKÝ, J.; JÍCHA, M. The influence of spill-line geometry on a spray generated by a pressure-swirl atomizer. In *EPJ Web of Conferences. EPJ Web of Conferences.* Praha, Czech Republic: 2015. ISSN: 2100-014X.

EPJ Web of Conferences **114**, 02070 (2016)
DOI: 10.1051/epjconf/201611402070


# The influence of spill-line geometry on a spray generated by a pressure-swirl atomizer

Milan Malý[1,a], Lada Janáčková[1], Jan Jedelský[1] and Miroslav Jícha[1]

[1]*Brno University of Technology, Faculty of Mechanical Engineering, Energy Institute, Technická 2896/2 Brno 616 69, Czech Republic*

**Abstract.** An experimental investigation of characteristics of spray generated by a pressure-swirl atomizer (spill-return type) was performed using shadowgraphy and Phase-Doppler Anemometry (PDA). Several different geometries of the spill-return orifice were tested in terms of a spray stability and quality on a cold test bench. PDA measurement yields a drop-size distribution and velocity data while the shadowgraphy unveils a break-up process in detail. Performed measurements reveal significant differences in spray characteristics as well as differences in spray stability. The results suggest that the air core, formed inside the swirl chamber, passes through the spill orifice, which causes instability of the inner flow. These instabilities lead to a chaotic state of sheet breakup resulting in shortening of breakup distance. Obtained findings are used to propose possible changes in the atomizer design for improvement of its performance.

## 1 Introduction

A spill-return atomizer is basically a pressure-swirl atomizer that contains a bypass in the swirl chamber known as a spill-line (SL) orifice. The liquid is injected via tangential ports to the swirl chamber, where it is divided into two streams, one of them is discharged outside and atomized, the second one is "spilled" back to the reservoir throught the SL orifice. The amount of spilled fuel is regulated by a control valve in a spill-line. Fuel is always supplied to the swirl chamber at high pressure providing good atomization over a wide span of injection flow rate. This feature allows using the spill-return atomizers in applications requiring the wide regulation range such as industrial burners and gas turbine combustors [1].

A number of studies focused on improvement of spray characteristics of pressure-swirl atomizers, but only a few of them were investigating spill-return atomizer and even less examined the influence of the spill-return orifice on the spray quality and stability. Nasr et al. in [2] tested several different diameters of spill orifice in terms of Sauter mean diameter (SMD) and flow rate. However, their atomizers were run with open spill line without any regulation, and the spill-feed ratio was controlled by a cross section of SL orifice. Our research is concentrated on test with regulated spill line along with closed spill line to simulate the full power of the atomizer.

Several small sized spill-return atomizers were chosen for this study varying only in the SL orifice geometry. Two different diameters of SL orifice were investigated with or without an obstacle blocking direct axial flow through the SL orifice. Also, several axial positions of the obstacle in the SL orifice were taken into account.

## 2 Experimental setup

Experiments were performed at a specially designed facility for cold spray generation under controlled conditions in the Spray laboratory at the Brno University of Technology.

### 2.1 Cold test bench

A schematic layout of the cold test bench is shown in Figure 1. It consists of a gear feed pump (3) that supplies fuel from a main tank (1) through filters (2), a flow meter (4), a pressure sensor (5), a temperature meter (7) and a control valve (8) into the atomizer (9). The spray falls into a collector and it is then returned to the main supply tank. The flow rate is controlled by a bypass needle valve (9). Spill-return line consist of a pressure sensor (6), a needle regulating valve (11) and a gear flow meter (12)

Flow rate in the fuel line is metered by Siemens Mass 2100 Di3 Coriolis mass flow meter fitted with a Mass 6000 transmitter. Flow rate uncertainty is 0.2 % of its actual value. The uncertainty of pressure sensors (BD Senzor DMP 331i) is 0.35 % of the actual value. The error of temperature sensor Omega PR-13 is 0.2 °C.

Operation regimes of the atomizer were controlled by setting the inlet pressure to 0.5, 1 and 1.5 MPa with the closed spill line by the valve near the atomizer. Spill mode of the atomizer was performed at an inlet pressure of 1 MPa with the spill-feed ratio of 0.4 and 0.8. The

[a] Corresponding author: milan.maly@vutbr.cz

spill-fill ratio is defined as the ratio of the amount of

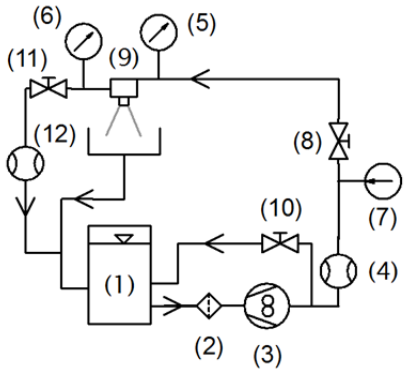


**Figure 1.** Schematic layout of the experimental facility

spilled fuel to the amount of pumped fuel to the atomizer

Kerosene Jet A-1 was used as the testing liquid. Physical properties of Jet A-1 at room temperature are: surface tension $\sigma = 0.029$ kg/s$^2$, dynamic viscosity $\mu_l = 0.0016$ kg/(m·s) and density $\rho_l = 795$ kg/m$^3$. All tests were done with one batch at 25 °C.

## 2.2 Phase Doppler anemometry

Droplet sizes and velocities were probed by two component Phase Doppler anemometer (PDA) Dantec Dynamics A/S, see a schematic layout in Figure 2. PDA measurement was made at an axial distance Z = 25 mm from the exit orifice. One radial profile with 31 positions was measured. In each position, 35,000 samples or 15 second long measurement were taken. Detailed setup information is summarized into Table 1.

Spray images were taken by Canon EOS D70 with Canon EF 100 mm f/2.8 UMS Macro lens fitted to 68 mm long extension tube. The spray was illuminated by Nd:YAG NewWave Research Gemini laser with a pulse duration of 5 ns and pulse energy of 5 mJ. The imaging system was configured to capture a shadowgraphy images.

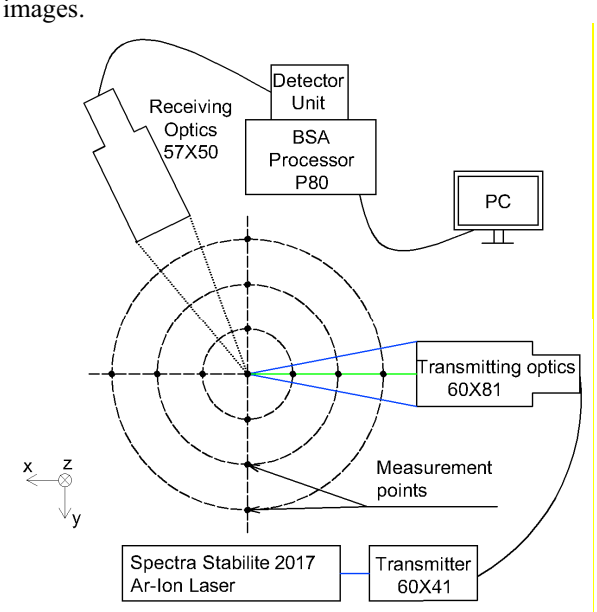


**Figure 2.** A setup of the PDA measurement

**Table 1.** PDA setup

| Parameter | Value |
|---|---|
| Laser power output | 1 W |
| Wavelength | 514.5 nm |
| Front focal length of transmitting optics | 310 mm |
| Front focal length of receiving optics | 800 mm |
| Scattering angle | 70° |
| Mask | B |
| Spatial filter | 0.050 mm |
| Velocity | Axial |
| Velocity center | 8 m/s |
| Velocity span | 32 m/s |
| Sensitivity | 800 V |
| SNR | 0 dB |
| Signal gain | 20 dB |
| Level validation ratio | 8 |

## 2.3 Tested geometries

Several small pressure-swirl atomizers with internal dimensions corresponding to
Figure 3 were investigated. Tested variations are listed in Table 2, where the B dimension represents a distance of the blocking obstacle from the top of the swirl chamber and $d_s$ a diameter of the SL orifice.

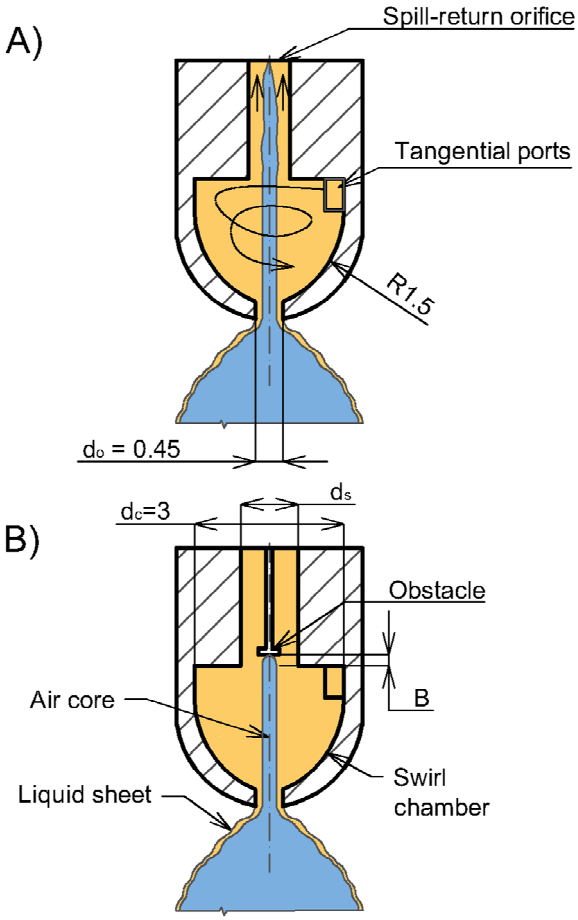


**Figure 3.** The geometry of the tested atomizer. A) Standard design (the SL orifice in the centre of the swirl chamber), B) Modified spill-line geometry with the obstacle

**Table 2.** Tested atomizers configurations

| Configuration | B [mm] | $d_s$ [mm] |
|---|---|---|
| **S1** | NA* | 0.8 |
| **S1B0** | 1 | 0.8 |
| **S1B2** | 3 | 0.8 |
| **S1B4** | 5 | 0.8 |
| **S2** | NA | 1.09 |
| **S2B0** | 1 | 1.09 |
| **S2B2** | 3 | 1.09 |
| **S2B4** | 5 | 1.09 |

*NA = Not applied

## 3 Results and discussion

The first part of this chapter focuses to the flow characteristics such as mass flow rate, discharge coefficient and overpressure in the spill line, the second one deals with the liquid breakup and the third one is concerning PDA measurements.

### 3.1 Discharge characteristics

Measuring of liquid mass flow through the atomizers exit orifice and pressure on the spill line (with closed spill line) shows unexpected results. As it is clear from Figure 4, liquid mass flow rate depends on the geometry of SL orifice even if the other dimensions remain unchanged. The lowest flow rate is almost the same for both SL orifice diameters (0.8 and 1.09 mm) with the obstacle closest to the swirl chamber. Moderate flow rate is achieved by 0.8 mm SL orifice, where the flowrate is the same for all positions of the obstacle (expect the closest one) as well as for atomizer without the obstacle. Only at 1.5 MPa, the S1B4 show much higher flow rate than it would be expected and the reason of it is still unexplained. The 1.09 SL orifice (except the S2B0) have the highest flow rates. A difference about 40 % in the mass flow rate between atomizers with and without obstacle shows a strong influence of SL orifice to the internal flow.

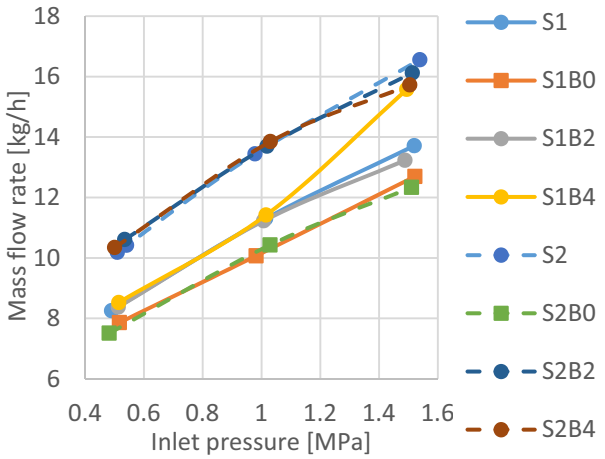


**Figure 4.** Mass flow rate with closed spill-line

Coefficient of discharge ($C_D$) is a ratio between the actual and the theoretical mass flow rate through the exit orifice, defined as:

$$C_D = \frac{\dot{m}_l}{A_0\sqrt{2\rho_l \Delta p}} \quad (1)$$

The $C_D$ is for pressure swirl atomizers usually low due to the presence of air core blocking off the central portion of the exit orifice and it is roughly independent on the inlet pressure. The $C_D$ values as a function of inlet pressure are shown in Figure 5 for all tested atomizers. Figure 4 indicates main trends of $C_D$ distribution over tested geometries. Atomizers with the obstacle closest to the swirl chamber have the lowest $C_D$ varying from 0.47 to 0.44. The highest $C_D$ was reached with 1.09 mm SL orifice diameter, changing from 0.64 to 0.57.

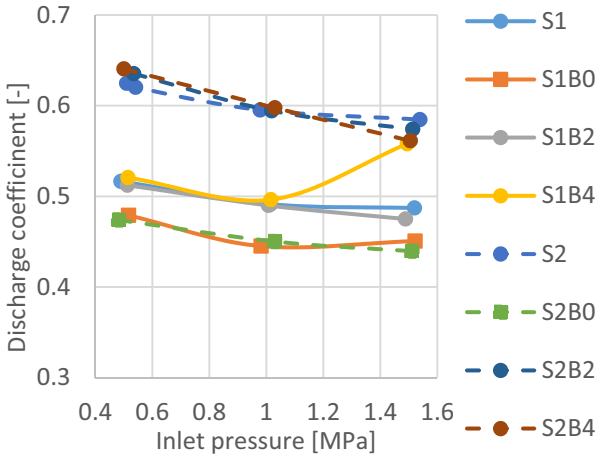


**Figure 5.** Discharge coefficient

A prediction of the discharge coefficient based on atomizer dimensions published by Rizk and Lefebvre in [3]:

$$C_D = 0.35\left(\frac{A_p}{d_s d_o}\right)^{0,5}\left(\frac{d_s}{d_o}\right)^{0,25} \quad (2)$$

gives $C_D = 0.39$ and it is independent on inlet pressure and SL orifice dimensions.

Lee et al. [4] report $C_D$ as a function of Reynolds number varying from 0.45 for high Re to 0.68 for low Re. They found a dependecy of air core stability on Re. Stable air core means a drop in the fuel flow rate as the center of the exit orifice is occupied by the air core.

Assuming that the air core created by internal swirl motion of tangentially injected liquid passes through the SL orifice, spill-return atomizer can be simplified into simple pressure-swirl type with extended swirl chamber. Influence of dimensions of the swirl chamber on internal flow was investigated by Kim et al. in [5]. They described a dependency of stability of the air core on the length of the swirl chamber, where longer swirl chamber lowers the air core stability. Taking these findings into account, we can assume that the geometries with the obstacle closest to the swirl chamber have stabilized the air core, while in the different configuration the air core is longer than its critical length and behave unstably, hence the $C_D$ and the mass flow rate increases.

The influence of spill-line pressure on the inlet pressure is revealed in Figure 6. As expected, SL pressure depends on the SL orifice diameter. The orifice with larger cross section has lower pressure losses and vice versa. But the obstacle in the spill line strongly increases the SL pressure (pressure drop is smaller). This behaviour is observed for both the SL orifice diameters it is attributed to the low $C_D$ value.

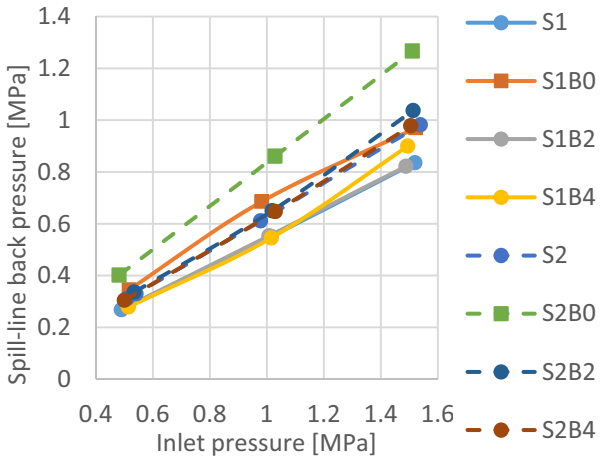


**Figure 6.** Spill-line back pressure

### 3.2 Liquid breakup

Droplet formation is a chaotic process, where discharged liquid sheet disintegrates due to aerodynamic forces between the liquid and stagnant surrounding air into filaments and ligaments and finally into drops in the form of a hollow cone spray. Longer breakup length would allow the liquid sheet to be thinned before the breakup and would result in smaller droplets. Entire breakup process is visualized in Figure 7. Images of the breakup process reveal how compact the liquid sheet is and if there are any long time instabilities.

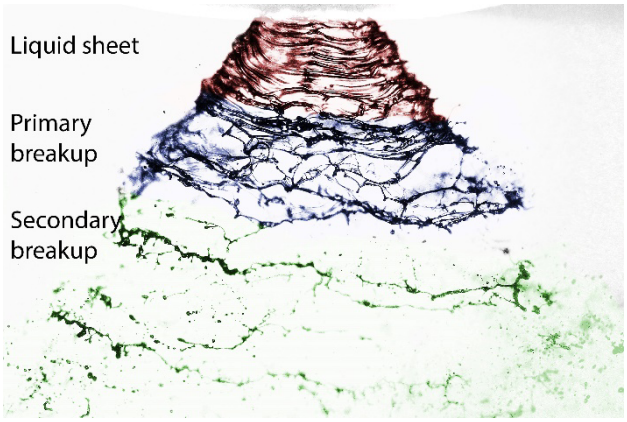


**Figure 7.** Near-nozzle spray structure

For detailed breakup, images see Figure 9. All tested configurations have in common that the breakup length strongly shortens with increasing inlet pressure, the atomizer S2B0 has the longest breakup length, which is most evident at $\Delta p = 0.5$ MPa and 1.0 MPa, while the S1B0 does not appear to have similar nature and behave the same way as the configurations without the obstacle. This is in contrary to the findings from the previous chapter, where both the atomizer have exactly the same $C_D$. Thus the same mode of the liquid break up was expected. Other atomizers (even those not shown in Figure 8) feature a chaotic breakup process where the liquid sheet is almost undetectable and very short. Short break up length might be linked to the instabilities of the air core that was predicted in the previous chapter.

### 3.3 Spray characteristics

Basic spray characteristics such as axial velocity profile, Sauter mean diameter profile or liquid mass distribution within the spray are evaluated at inlet overpressure 1 MPa with closed spill line. .The configurations with the obstacle placed further from the exit orifice were omitted from the PDA measurements.

The radial distribution of the mean droplet axial velocity corresponds well to other observations of hollow cone sprays for the case of atomizers with the obstacle (see Figure 8), where axial velocity reaches a local maximum at approx. 16 mm from the spray centre. Geometries without the obstacle have this maximum much less distinct. Velocities in the spray centre are divided by the diameter of SL orifice, where 1.09 mm orifice (both, with and without the obstacle) have by 25% higher axial velocity than 0.8 mm orifice.

The SMD is lower for atomizers with the obstacle in the spray centre (see Figure 10). The difference between S1 and S1B0 is modest in all radial distances, however S2 have 2.5 times higher SMD in the centre compared to the same geometry with the obstacle (S2B0) which has the lowest SMD in almost every position.

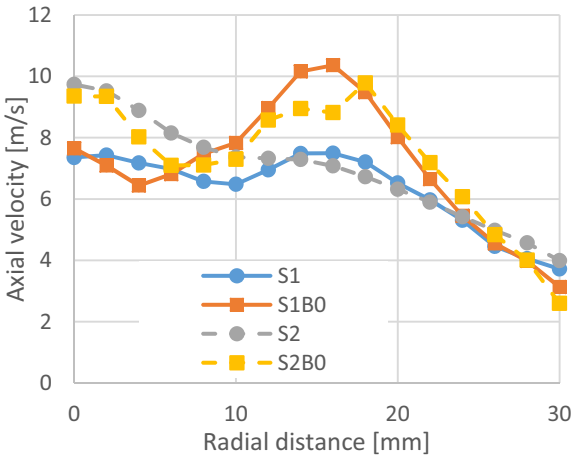


**Figure 8.** Axial velocity for $\Delta p = 1$ MPa with closed spill line

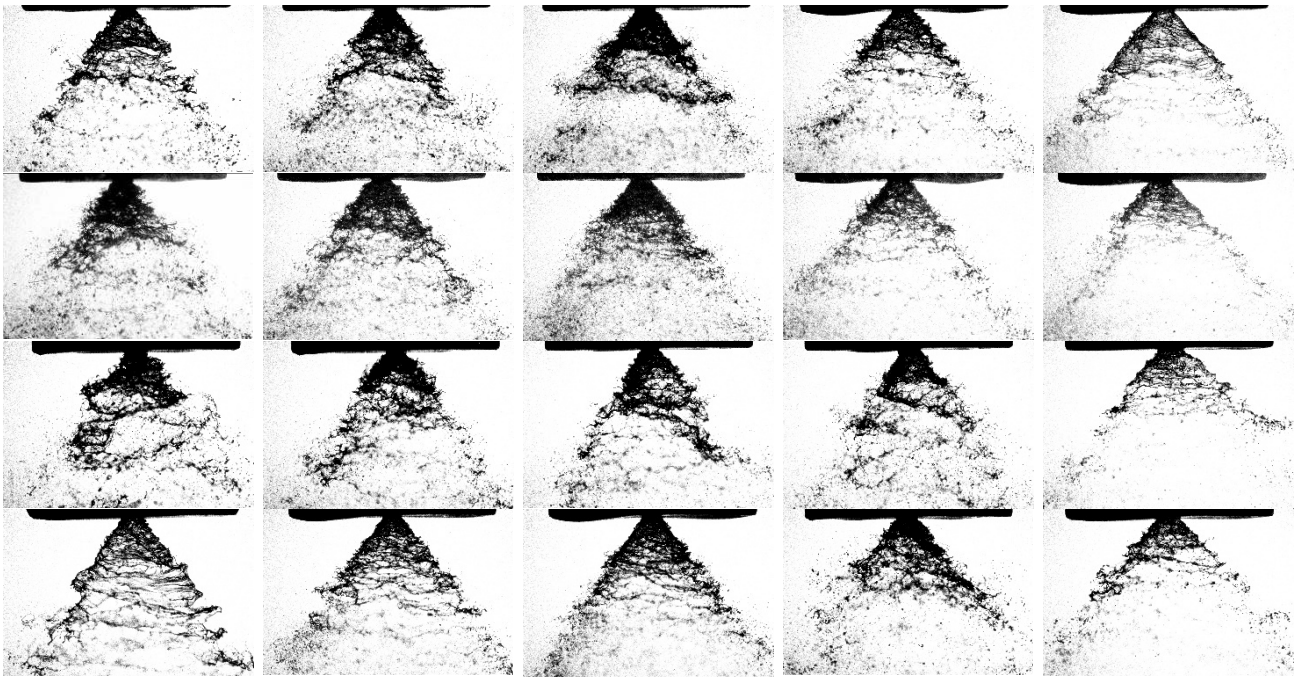

**Figure 9.** Liquid breakup visualization. Columns: from left $\Delta p$ = **0.**5, 1, 1.5 MPa with SFR 0; 1 MPa SFR 0.4 and 1 MPa SFR 0.8. Rows from top: S1, S1B0, S2, and S2B0. The size of each photograph is 7x10 mm.

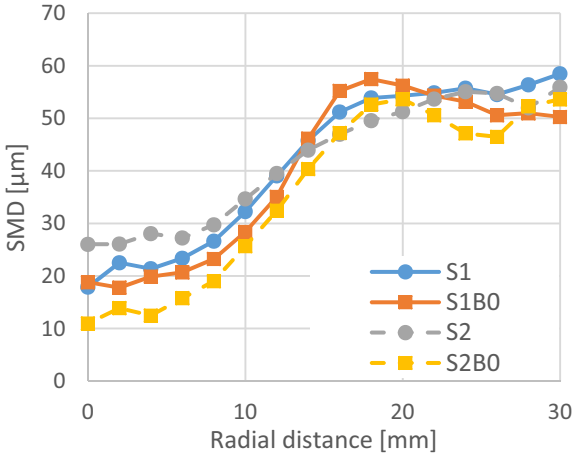


**Figure 10.** SMD for $\Delta p$ = 1 MPa with closed spill line

Cumulative liquid mass distribution in Figure 11 reveals significant divergence between the configurations with and without the obstacle. S1B0 and S2B0 have more liquid concentrated at positions further from spray centreline – where an annular liquid sheet is expected. Atomizers without the obstacle have concentrated about 37% of entire liquid mass flow at radial distance of 11 mm while the atomizers with the obstacle only 16% thus the mass distribution of S1 and S2 does not fully correspond to the idea of hollow cone spray.

This observation together with findings from Figure 8 indicate a problem of the liquid sheet stability that was confirmed by the breakup visualization in Figure 9.

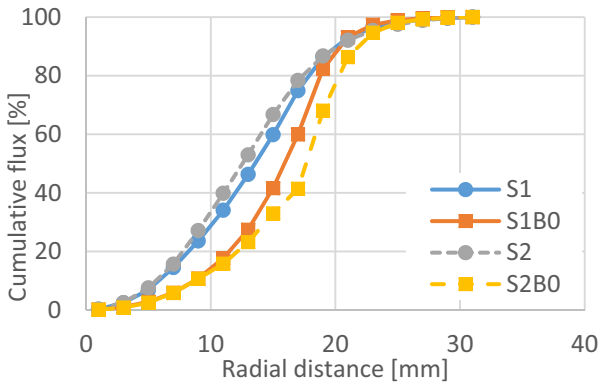


**Figure 11.** Liquid mass distribution $\Delta p$ = 1 MPa

For evaluation of inlet pressure influence on SMD a global form of the SMD was calculated:

$$ISMD = \frac{\sum_{i=1}^{N_i} n_i f_i D_i^3}{\sum_{i=1}^{N_i} n_i f_i D_i^2} \quad (3)$$

As shown in Figure 12, with increasing pressure the ISMD decreases for all tested atomizers. The highest ISMD in the whole tested range is attributed to the S1B0 while the S2B0 has about 10% lower ISMD. Both atomizers have the same $C_{D,}$ but the disparity in their ISMD confirms a different breakup mode showed in Figure 9. The lowest ISMD at 0.5 MPa was reached by the S2B0 as it was predicted by the visualization (the longest breakup) however the S2 has the lowest ISMD at the rest of the tested regimes.

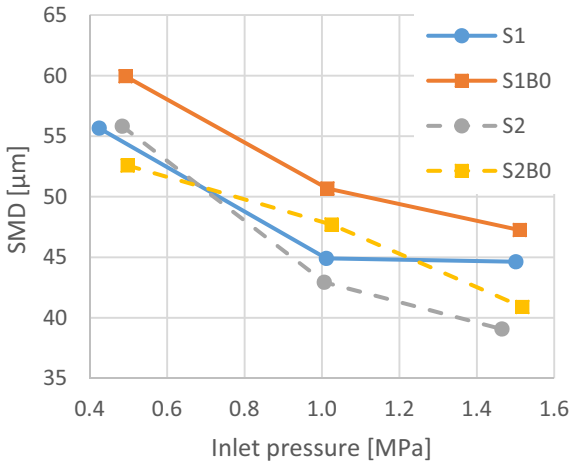


**Figure 12.** Global SMD as function of inlet pressure

## 4 Conclusion

The study of the influence of various SL orifice on spray was focused on discharge characteristics, near nozzle liquid break up and spray quality in terms of liquid distribution and SMD. Discharge coefficient of the flow through the exit orifice was found dependent on the diameter of SL orifice and also on the obstacle presence. A question of the air core instabilities caused by air core passing through the SL orifice were discussed with other related publications.

Spray visualization shows very short and chaotic breakup except the atomizer with the obstacle close to the swirl chamber and large diameter of SL orifice.

The spray structure was described based on spatially resolved velocity, drop size and mass flux. Different radial distributions of axial velocity indicate a problem with the hollow cone liquid sheet formation in the case of atomizers without the obstacle which is also confirmed by the analysis of liquid mass distribution across the spray diameter.

This study is a brief introduction to the problem of the influence of SL orifice geometry on the spray characteristics and reveals the importance of proper SL orifice design. Further investigation with a focus on the internal flow shows its necessity due to a lack of published papers dealing with phenomena.

## Acknowledgement

This work has been supported by the project No. GA15-09040S funded by the Czech Science Foundation, the project LO1202 NETME CENTRE PLUS with the financial support from the Ministry of Education, Youth and Sports of the Czech Republic under the "National Sustainability Programme I" and project Reg. No. FSI-S-14-2355 funded by the Brno University of Technology.

## References

1. A. H. Lefebvre, *Atomization and sprays* (1989)
2. G. Nasr, A. Yule, and S. Lloyd, *ILASS* (2007)
3. N. K. Rizk, and A. H. Lefebvre, Journal of Propulsion and Power, **1**, 193-199 (1985)
4. E. J. Lee, S. Y. Oh, H. Y. Kim., Experimental thermal and fluid science, **34**, 1475-1483 (2010)
5. S. Kim, T. Khil, D. Kim, Measurement Science and Technology, **20** (2009)

# C. Conference paper at AEaNMiFME 2016

**Reference:**

MALÝ, M.; JANÁČKOVÁ, L.; JEDELSKÝ, J.; JÍCHA, M. Effects of Alternative Fuel Characteristics on Spray Generated by Small Pressure-Swirl Atomizer. *The Application of Experimental and Numerical Methods in Fluid Mechanics and Energy Conference Proceedings 2016.* Těrchová, Slovakia: Faculty of Mechanical Engineering University of Žilina, 2016. s. 121-125. ISBN: 978-80-554-1193-4

**AEaNMiFMaE 2016, 27-29 April 2016**
University of Žilina, Department of Power Engineering,
Žilina, Slovakia

# Effects of alternative fuel characteristics on spray generated by small pressure-swirl atomizer

Milan Malý*, Lada Janáčková*, Jan Jedelský*, Miroslav Jícha*
*Brno University of Technology, Faculty of Mechanical Engineering, Energy Institute, Technická 2896/2, 61669 Brno, Czech Republic , milan.maly@vutbr.cz

A B S T R A C T
*A systematic investigation was made on the differences in atomizing performance among several crude-oil based fuels and water in a small pressure-swirl atomizer. The atomizer performance is characterized in terms of discharge coefficient, Sauter mean diameter and nozzle efficiency. Phase-Doppler anemometry was used to document the mean structure of the developed spray and provides information about droplets sizes and velocities. A strong dependence of liquid viscosity on the mass flow rate through the atomizer as well as on the spray quality was found and discussed with relevant literature.*

***Keywords:***
Pressure-swirl, atomization, kerosene, diesel, water

## 1. Introduction

The atomizers, which are used to deliver sprayed fuel into gas turbine combustion chamber, are routinely tested to determine whether their performance meets specifications both for flow rates and a spray quality. In this article we evaluate the possibility of kerosene Jet-A1replacement by alternative fuels such as arctic and winter diesel or by renewable fuels like diesel with biological additive or refined palm oil. Beside standardized petroleum fuels, water and light heating oil (LHO) take their place in order to expand the range of liquid properties.

Pressure-swirl (PS) atomizers convert pressure energy of pumped liquid into kinetic and surface energy of final droplets. The liquid is first injected via tangential ports inside a swirl chamber where it gains a swirl motion under which it leaves an exit orifice in form of an annular liquid sheet. This sheet breaks up due to aerodynamic forces between the liquid and stagnant surrounding air – see Fig 2a). This process is strongly influenced by the internal flow as well as by the liquid properties.

## 2. Experimental setup

Experiments were performed at a specially designed facility for spray generation under controlled conditions in the Spray laboratory at the Brno University of Technology. The experimental apparatus includes an atomizer under test, cold test bench with liquid supply system, and Phase-Doppler anemometry (PDA).

### 2.1. Cold test bench and tested atomizer

A schematic layout of the test bench is shown in Fig 1a). The liquid is fed by a gear pump (3) through filter (2), flow meter (4) and control valve (6) into the atomizer (8). The spray falls into a collector and then it is returned to the main supply tank (1). The flow rate is regulated by a bypass needle valve (11). Flow rate is metered by Siemens Mass 2100 Di3 Coriolis mass flow meter fitted with a Mass 6000 transmitter. Flow rate uncertainty is 0.2 % of its actual value. The feeding line is also equipped with pressure (7) and temperature sensors (5). Uncertainty of pressure sensor (BD Senzor DMP 331i) is 0.35 % of its actual value. A tested atomizer (schematically shown in Fig 2b) is a small PS of spill-return type. A spill-line equipped with a pressure sensor (9) was closed by valve (10) near the atomizer. All tests were done at inlet overpressure of 1 MPa.

### 2.2. Phase Doppler anemometry

Characteristics of the sprayed droplets (time-resolved droplet size and velocity) were measured using two-component Fiber PDA made by Dantec Dynamics A/Sand; its configuration with coordinate system is shown in Fig 1b). PDA measurements were conducted in three radial sections of the spray at axial distances of Z = 5, 25 and 50 mm from the atomizer exit orifice. Twenty one positions were measured at each axial distance in one axis. In each position, 16,384 samples or 30 seconds were taken.

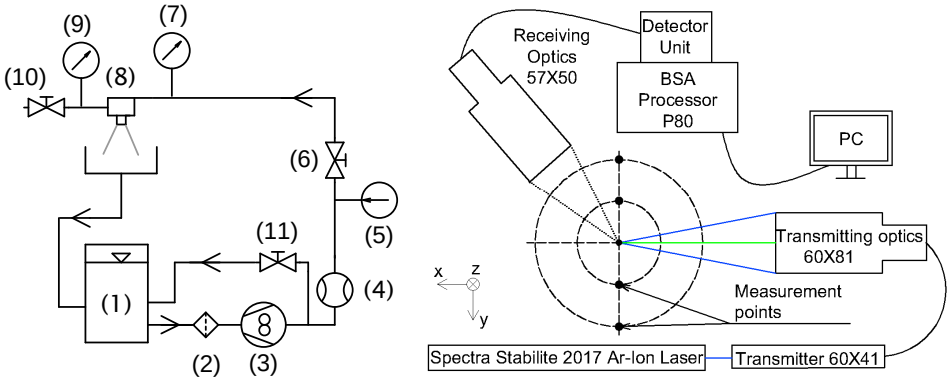


**Fig. 1** a) Experimental test bench (left) b) PDA setup (right)

### 2.3. Tested liquids

The physical properties of tested liquids are listed in Tab. 1 for the temperature (20 °C) normally used in tests. It should be noted that all crude oil-based liquids have a surface tension very similar to each other while water has a surface tension about 2.5 times higher.

**Tab. 1** Fuel properties and mass flow rates at overpressure Δp = 1 MPa

| Liquid | Density $\rho_l$ [kg/m$^3$] | Kinematic viscosity $\nu_l$ [mm$^2$/s] | Dynamic viscosity $\mu_l$ [mPa·s] | Surface tension $\sigma_l$ [mN/m] | Mass flow rate $\dot{m}_l$ [kg/h] | $C_D$ [-] |
|---|---|---|---|---|---|---|
| **Kerosene** | 785 | 1.5 | 1.9 | 31 | 16.8 | 0.45 |
| **Arctic diesel** | 810 | 2.6 | 3.2 | 29 | 18.9 | 0.49 |
| **Winter diesel** | 830 | 3.7 | 4.4 | 23 | 19.8 | 0.51 |
| **Biodiesel** | 831 | 3.9 | 4.6 | 27 | 19.8 | 0.51 |
| **Palm oil** | 771 | 4 | 5.2 | 29 | 19.4 | 0.52 |
| **LHO** | 885 | 17 | 19.2 | 35 | 25.6 | 0.64 |
| **Water** | 997 | 1.1 | 1.1 | 71 | 18.0 | 0.42 |

## 3. Results and discussion

The first part focuses on discharge characteristics and the second deals with the developed spray.

### 3.1. Discharge parameters

A discharge behavior for our atomizer at the given pressure is shown in Tab. 1 and graphically illustrated in Fig. 4. The obvious fact that can be understood as counter-intuitive is that a liquid with higher viscosity provides a significantly higher mass flow rate than a less viscous fluid. In order to eliminate the influence of the liquid density, the discharge coefficient $C_D$ was calculated as follows:

$$C_D = \frac{\dot{m}_l}{\dot{m}_{teor}} = \frac{\dot{m}_l}{A_o\sqrt{2\rho_l \Delta p}} \qquad [-] \qquad (1)$$

where $A_o$ is the area of exit orifice. In commonly used empirical correlations, liquid viscosity has a small influence (Jones [1] $C_D \sim \mu_l^{0.02}$) or non-influence (Rizk [2]) on $C_D$; however these studies were done for a larger scale atomizer. A more recent study by Wimmer [3] derived a theoretical correlation for the liquid flow rate as (inter alia) a function of dynamic viscosity where $\dot{m}_l \sim \mu_l^{0.115}$ ,which was subsequently confirmed by experiments. However, in our study, the atomizer with the area of the exit orifice more than two times smaller is used, resulting in $C_D \sim \mu_l^{0.15}$ with coefficient of determination $R^2 = 0.99$. This entire phenomenon is caused by decrease in the inner air core diameter that results in increase in the flow cross-section through the exit orifice [3]. Nevertheless, $C_D$ does not match the values predicted by [1, 2]. This difference was discussed in [4] and it is attributed to the presence of the spill-line orifice which causes minor spray fluctuations and consequently affects the inner air core.

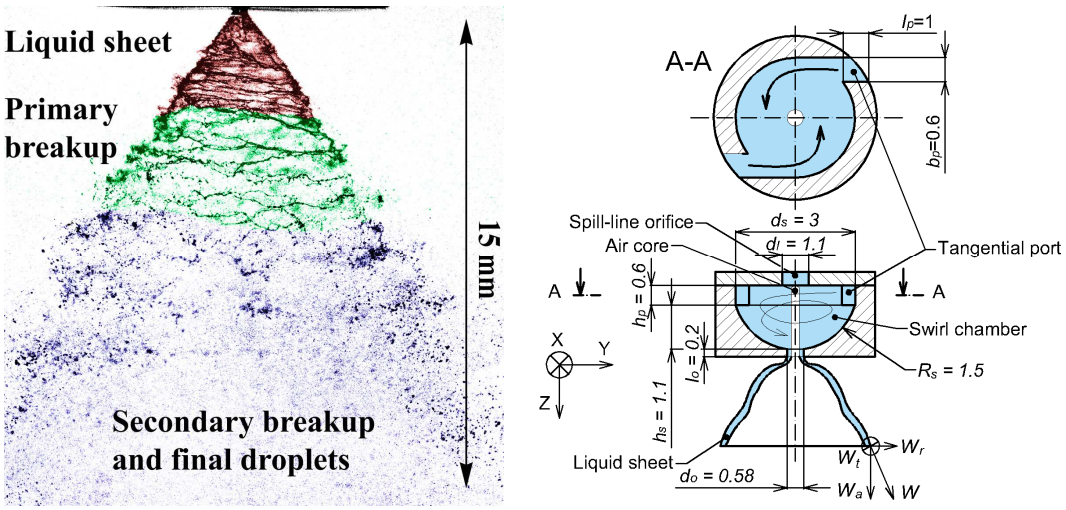


**Fig. 2** a) Spray development at Δp = 1 MPa, b) Atomizer schematic drawing

The efficiency of energy conversion is another important quantity describing the efficiency of conversion of pressure energy into the kinetic energy of liquid structures and is defined as $\eta_n = \rho_l w_o^2 / 2\Delta p$ ,where $w_o^2$ is the velocity at the atomizer exit orifice and was estimated by approximating our PDA data. In our case $\eta_n$ = 29–53 % and is strongly correlated ($R^2$ = 0.90) with liquid viscosity – see Fig. 4a).

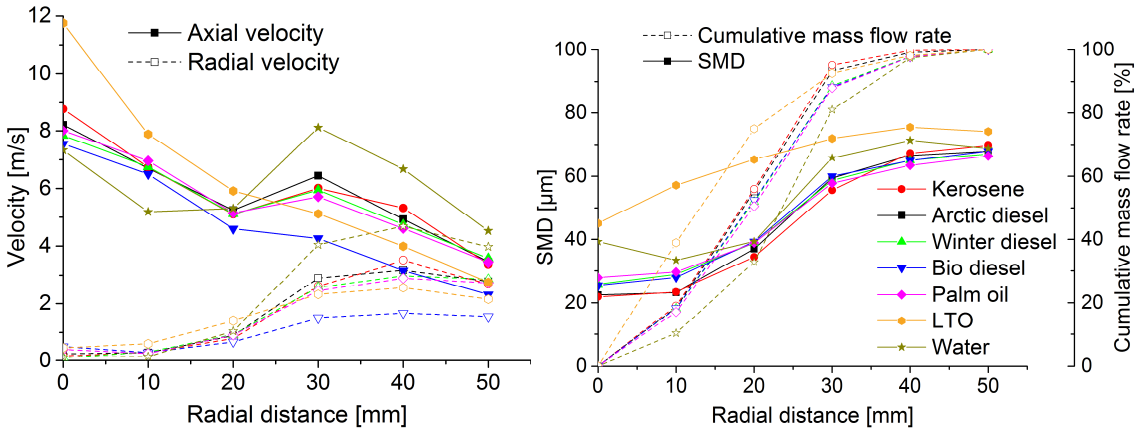


**Fig. 3** a) Spray velocities profiles b) SMD and flow rate profiles

## 3.2. Spray characteristics

The radial distribution of liquid mean velocity (Fig 3a) well corresponds to other observation of hollow-cone sprays; a local maximum is expected in positions where the annular liquid sheet disintegrated, expect for LHO that provides a much higher velocity in the spray center which almost linearly decreases with increasing radial distance. Along with the findings from Fig 3b), where LHO has a considerably higher SMD in the regimes near the spray center and the liquid distribution shows a rather full-cone spray, it may be considered that the internal air core collapsed in the same way as it was described in [3] for high viscous liquids. Due to small differences in the spray characteristics of petroleum-based fuels, it is convenient to use a global characteristic describing the whole spray by one number. From the PDA data, integral SMD (ISMD) [5] was calculated at axial distances of 25 and 50 mm from the atomizer and the estimated spray cone angle (SCA) as the limit, where 90 % of the liquid volume is inside the spray. In comparison with the kerosene, all alternative fuels have about 7–11 % higher ISMD. A correlation between ISMD and the liquid viscosity for both axial distances is shown in Fig 4b); water is excluded due to a significantly higher surface tension. ISMD depends on the liquid viscosity as ISMD ~ $\mu_l^{0.16}$ for Z =25 mm with $R^2$ = 0.93 and ISMD ~ $\mu_l^{0.15}$ for Z =50 mm with $R^2$ = 0.96. Published data (reviewed in [6]) reported several correlations varying from ISMD ~ $\mu_l^{0.118}$ to ISMD ~ $\mu_l^{0.25}$ in dependence on the used atomizers and liquids. It is also worth mentioning that ISMD grows with increasing axial distance. This behavior was attributed to droplets coalescence and evaporation [7].

**Tab. 2** PDA data

| Liquid | ISMD* [µm] | ISMD** [µm] | SCA** [deg] | Nozzle efficiency $\eta_n$ [-] |
|---|---|---|---|---|
| **Kerosene** | 41.2 | 47.3 | 60 | 0.42 |
| **Arctic diesel** | 44.2 | 50.6 | 60 | 0.40 |
| **Winter diesel** | 45.2 | 52.1 | 64 | 0.38 |
| **Biodiesel** | 44.9 | 52.7 | 65 | 0.35 |
| **Palm oil** | 44.1 | 51.6 | 65 | 0.37 |
| **LHO** | 59.0 | 65.7 | 59 | 0.29 |
| **Water** | 51.5 | 62.0 | 71 | 0.53 |

*Calculated for Z = 25 mm **Calculated for Z = 50 mm

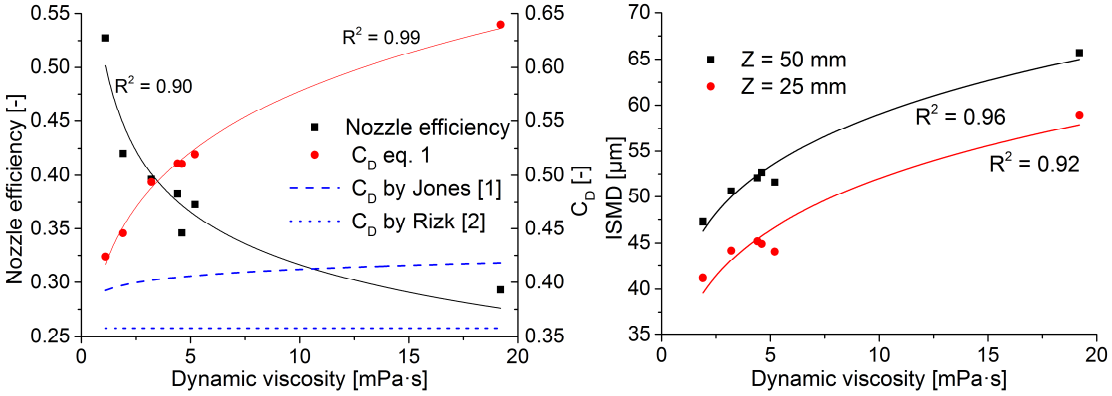


**Fig. 4** a) Correlation between the nozzle efficiency and discharge coefficient b) ISMD correlation (water excluded)

# 4. Conclusion

Several liquids were tested and their influence on discharge parameters and spray characteristics were discussed. A significant impact of the liquid viscosity on the liquid mass flow rate appeared to be an important parameter to be taken into account provided that the kerosene is to be replaced by the alternative fuels. These fuels have about 13–18 % higher throughput and also about 7–11 % higher SMD. A correlation between SMD and the liquid viscosity was also established and briefly discussed with relevant literature.

# Acknowledgement

This work has been supported by the project No. GA15-09040S funded by the Czech Science Foundation and the project LO1202 NETME CENTRE PLUS with the financial support from the Ministry of Education, Youth and Sports of the Czech Republic under the "National Sustainability Programme I".

# References

[1] Jones, A. *Design optimization of a large pressure-jet atomizer for power plant*. Proceedings of the Second International Conference on Liquid Atomization and Spray Systems, 1982

[2] Rizk, N. K., and Lefebvre, A. H. *Internal flow characteristics of simplex swirl atomizers.* Journal of Propulsion and Power, 1985.

[3] Wimmer, E., and Brenn, G. *Viscous flow through the swirl chamber of a pressure-swirl atomizer*. International Journal of Multiphase Flow, 2013

[4] Maly, M., Janackova, L., Jedelsky, J., and Jicha, M. *The influence of spill-line geometry on a spray generated by a pressure-swirl atomizer*.EPJ Web of Conferences, in press

[5] Jedelsky, J., and Jicha, M.*Energy considerations in spraying process of a spill-return pressure-swirl atomizer*. Applied Energy, 2014

[6] Lefebvre, A. *The prediction of Sauter mean diameter for simplex pressure-swirl atomisers*. Atomisation Spray Technology, 1987

[7] Chin, J., Nickolaus, D., and Lefebvre, A. *Influence of downstream distance on the spray characteristics of pressure-swirl atomizers*. Journal of engineering for gas turbines and power, 1986